

UNIVERSITY OF TARTU
FACULTY OF SCIENCE AND TECHNOLOGY
INSTITUTE OF MOLECULAR AND CELL BIOLOGY
INSTITUTE OF BIOMEDICINE AND TRANSLATIONAL MEDICINE
DEPARTMENT OF PHARMACOLOGY

**Selecting endpoints to use in preclinical trials in a mouse model of
Alzheimer's disease**

Bachelor thesis (12 EAP)

Jana Aid

Supervisor: Miriam A Hickey, PhD

Co-supervisor: Tambet Tõnissoo, PhD

TARTU 2021

Selecting endpoints to use in preclinical trials in a mouse model of Alzheimer's disease

Alzheimer's disease (AD) is a neurodegenerative disorder of the brain, that leads to cognitive impairment. AD is characterised by the accumulation of β -amyloid peptides and tau proteins into amyloid plaques and neurofibrillary tangles. AD currently has no cure, however promising research and treatment is underway. The aim of this work is to determine appropriate endpoints to use in a preclinical trial of 5xFAD mouse model of AD. In this thesis, I demonstrate endpoints appropriate to use for preclinical trials and appropriate group and effect sizes.

KEYWORDS: Alzheimer's disease, 5xFAD, microglia, histology

CERCS code: B640 Neurology, neuropsychology, neurophysiology

Prekliinilistes uuringutes kasutatavate tulemusnäitajate valimine Alzheimeri tõve hiiremudelis

Alzheimeri tõbi on aju neurodegeneratiivne haigus, mis põhjustab kognitiivseid probleeme. Seda iseloomustab β -amüloid valgu agregaatide moodustumine ja neurofibrillaarsed tängud. Alzheimeri tõvele tänaseni ravi puudub, kuid paljutõotavad uuringud ja potentsiaalsete ravimikandidaatide testimised on käimas. Bakalaurusetöö eesmärk on määrata sobilikud tulemusnäitajad, mida oleks võimalik kasutada prekliinilistes uuringutes kasutades 5xFAD Alzheimeri hiiremudelit. Antud töö tulemusena selgitasin välja milliseid tulemusnäitajaid on sobiv kasutada prekliinilises uuringus ning leian selleks sobivad grupi ja toime suurused.

MÄRKSONAD: Alzheimeri tõbi, 5xFAD, mikroglia, histoloogia

CERCS kood: B640 Neuroloogia, neuropsühholoogia, neurofüsioloogia

CONTENTS

LIST OF ABBREVIATIONS	5
INTRODUCTION	6
1.LITERATURE REVIEW	7
1.1 Overview of Alzheimer’s disease	7
1.2 Symptoms and diagnosis	8
1.3 Treatments	10
1.4 Pathology in Alzheimer’s disease	11
1.4.1 Gross pathology	11
1.4.2 Microscopic pathology	12
1.4.2.1 Amyloid and tau pathology in Alzheimer’s disease	12
1.4.2.2 Neuroinflammation in AD	14
1.5 Transgenic mouse models of Alzheimer’s disease	14
1.5.1 Overview of mouse models	14
1.5.2 5XFAD mouse model	15
1.5.3 Pathology in 5xFAD mouse model	16
1.5.4 Preclinical trials in AD	17
2.EXPERIMENTAL PART	18
2.1 The aims of the work	18
2.2 Materials and methods	18
2.2.1 Animals.....	18
2.2.2 Behavioural analysis.....	19
2.2.3 IBA1 antibody immunostaining for the pilot trial	19
2.2.4 Preclinical trial.....	20
2.2.4.1 Brief protocol of preclinical trial	21
2.2.5 Analysis of percent area using ImageJ	21
2.2.6 Particle analysis using ImageJ.....	22
2.2.7 Statistics.....	23
2.3 Results and discussion	23
2.3.1 Behavioural analysis.....	23
2.3.2 Percent area based upon IBA1 immunostaining.....	24
2.3.2.1 Power analysis of percent area.....	27
2.3.3 Particle analysis based upon IBA1 antibody immunostaining	28
2.3.3.1 Power analysis based on the results of the particle analysis.....	30
2.4 Preclinical trial.....	31
2.4.1 Percent area from the preclinical trial.....	31
2.4.2 Particle analysis for the preclinical trial	33

CONCLUSION	34
KOKKUVÕTE	35
REFERENCES	37
INTERNET REFERENCES	46
ACKNOWLEDGMENTS	47
NON-EXCLUSIVE LICENCE	48

LIST OF ABBREVIATIONS

5xFAD- 5x familial AD

A β - β -amyloid

AD- Alzheimer's disease

APOE ϵ 4- apolipoprotein E

APP- amyloid precursor protein

CT- computed tomography

DAB-3-3diaminobenzidine

DAM- disease-associated microglia

fAD- familial AD

FDG- fluorodeoxyglucose

IBA1- ionized calcium binding adaptor molecule 1

m- months

MCI- mild cognitive impairment

MRI- magnetic resonance imaging

mRNA- micro ribonucleic acid

NFcur- nanoformulated curcumin

ns- not significant

PBS- phosphate buffered saline

PET- positron emission tomography

PS1- presenilin 1

PS2- presenilin 2

RNA- ribonucleic acid

TB- tris buffer

TG- transgenic

TX- triton

WT- wild type

INTRODUCTION

Alzheimer's disease (AD) is a complex neurodegenerative disease with a slow progression. It is the main cause of dementia and is characterised by memory impairment and progressive neurocognitive dysfunction. The two main histopathological characteristics of AD are the extracellular amyloid plaque, formed by β -amyloid protein aggregates, and intracellular neurofibrillary tangles, made of hyperphosphorylated tau proteins. Both of these cause neuroinflammation in the brain. The aggregation of the plaques further leads to the activation of microglia cells, phagocytes in the central nervous system, that are crucial for maintaining homeostasis by removing damaged neurons and infection. However, in AD microglia cells over time become incapable of clearing the toxic amyloid plaques, which contributes to neurotoxicity and neurodegeneration (Tiwari et al., 2019; Kinney et al., 2018).

AD currently has no cure and the majority of therapeutic targets tested are focused on β -amyloid and tau, with the goal of reducing their aggregation to reduce their neurotoxicity. However, this research has not led to any major breakthroughs, which is why identifying new strategies based on other mechanisms could increase the chance of finding effective therapy. Critically, preclinical research and experiments should be completed with appropriate endpoints, group sizes and effect sizes (Egan & Macleod, 2014).

The theoretical part of this thesis provides an overview of the pathology involved in AD and gives an overview of current research and testing of treatments, thereby shining a light onto problematic areas in preclinical trials. Our research group is investigating the effect of nanoformulated curcumin on Alzheimer's disease in 5xFAD mice and thus appropriate endpoints and tests need to be chosen for a successful preclinical trial. The experimental part of this thesis is to determine the best endpoints to use in the preclinical trial by determining appropriate behavioural endpoints, group sizes and effect sizes. From the results of this work appropriate endpoints can be used for the preclinical trial without wasting time or resources on unnecessary testing and analysis. The analysis of the preclinical trial with nanoformulated curcumin could suggest whether using this drug could have an effect on the prevention of neurodegeneration associated with AD.

The experimental part of this thesis was performed at the Institute of Biomedicine and Translational Medicine in the Department of Pharmacology at University of Tartu.

1.LITERATURE REVIEW

1.1 Overview of Alzheimer's disease

Alzheimer's disease (AD) is a progressive neurodegenerative disease, that is characterised by the accumulation of β -amyloid and tau proteins into amyloid plaques and neurofibrillary tangles, respectively, that are associated with cognitive problems including memory impairment (Weiner et al., 2015). AD is typically a disease of the elderly, indeed, increasing age is the strongest risk factor and risk increases with increasing age. An estimated 1 out of every 10 older individuals (65+ years) are affected by dementia, and AD is the most common type at approximately 75% of all cases. Approximately 5 million new cases of AD are diagnosed every year (Qiu et al., 2009). It is estimated that 50% of people at the age of 85 face the risk of developing AD (Zhao et al., 2014).

Although patients with AD typically notice cognitive symptoms during older age, the amyloid starts building up in the brain years in advance (Fig. 1). Tau however develops closer to the onset age. The amyloid-cascade hypothesis predicts that the changes in β -amyloid pathology can further lead to changes in tau pathology. Nonetheless these changes initially start in different areas of the brain, which is inconsistent with the hypothesis and has been called the spatial paradox (van der Kant et al., 2020).

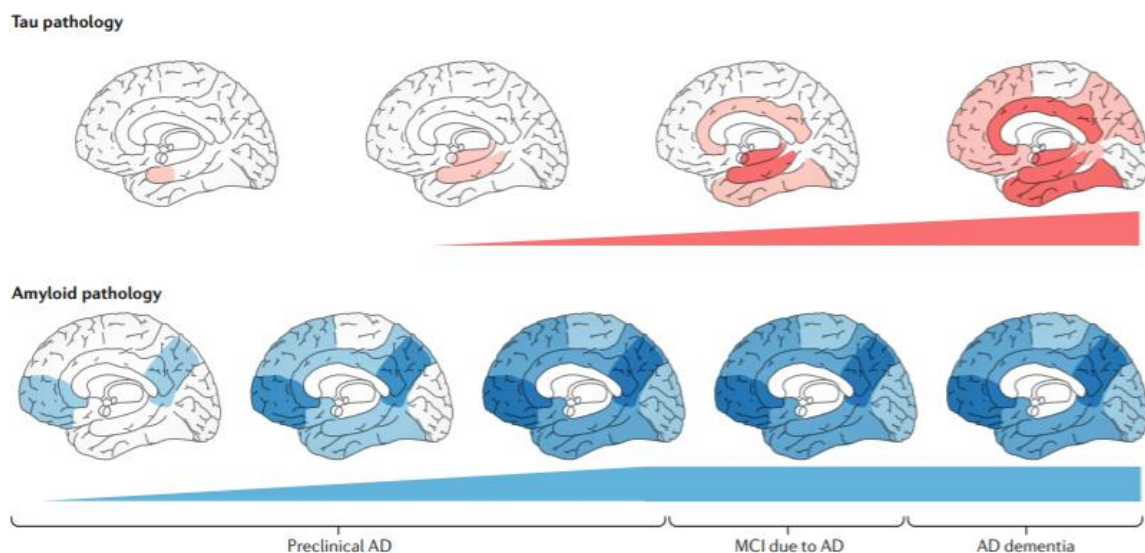


Figure 1. Progression of β -amyloid and tau accumulation in AD. Simplified overview of amyloid and tau pathology from neuropathology and positron emission tomography (PET) studies. The red areas show the areas of the brain affected by tau during different stages of AD and blue areas show the areas of the brain affected by amyloid pathology. MCI- mild cognitive impairment. This figure shows extensive amyloid pathology already in the preclinical stage of AD, while tau accumulates later. This figure also shows that the accumulation starts in different areas of the brain (Adapted from van der Kant et al., 2020).

There are 2 types of Alzheimer’s disease- sporadic and familial, which are divided into early-onset and late-onset and both have a genetic component. Variants of these genes can lead to an increased risk of developing AD (thus, they are a risk factor) or cause AD (disease-causing mutation). All of these genes are located on different chromosomes and are associated with either sporadic inheritance (thus, risk factor) or autosomal dominant inheritance (disease-causing mutations; Table 1). Late-onset sporadic AD is the more common type of AD, with an age at onset later than 65 years. Research has found that a specific polymorphism of the apolipoprotein E gene (APOE ϵ 4 allele) increases a person’s risk of developing late-onset sporadic AD, thus making it a risk factor. The APOE gene is located on chromosome 19 and having 1 allele of APOE ϵ 4 already increases the risk of amyloid deposition and onset of AD. However not everyone who inherits the APOE ϵ 4 develops AD (Jansen et al., 2015, Bekris et al., 2010).

Early-onset (familial) AD (fAD) is rare and accounts for around 1%- 6% of all AD cases. Clinical symptoms of fAD can already appear at very young age (before the age of 65, usually after the age of 30). There are 3 single genes that carry, disease-causing, fAD mutations: amyloid precursor protein (APP) on chromosome 21, presenilin 1 (PS1) on chromosome 14 and presenilin 2 (PS2) on chromosome 1. Mutations that occur in these genes result in the production of abnormal proteins that are associated with AD (Bekris et al., 2010; Bird, 2008). These mutations have been recreated in transgenic models, to create mouse models with construct validity, e.g., the 5xFAD mouse model, which expresses transgenes for APP and PSEN1 carrying 3 and 2 fAD mutations, respectively (Oakley et al., 2006).

Table 1 Genes associated with Alzheimer’s disease.

	Gene		Inheritance	Example mutation	Chromosome
Late-onset AD	Apolipoprotein E	APOE	Sporadic	-	19
Early-onset AD	Amyloid precursor protein	APP	Autosomal Dominant	V717I (London)*	21
	Presenilin 1	PS1	Autosomal Dominant	M146L**	14
	Presenilin 2	PS2	Autosomal Dominant	N141I***	1

*Eckman et al., 1997; **Sherrington et al., 1995; ***Levy-Lahad et al., 1995

1.2 Symptoms and diagnosis

The early symptoms of AD patients include memory impairment, difficulties in executing daily life activities and withdrawal from social life. There is also atypical presentation, which is often not recognised, which include progressive decline in attention, languages, and spatial reasoning. With disease progression and rapid decline in memory, changes in mood can occur, which can lead to difficulty in social situations (Scheltens et al., 2016; Zhao et al., 2014).

Diagnosing a patient suspected of having AD consists of three parts. The first one is based on clinical history from a reliable informant, that contains the general medical history, family history, neurological and neuropsychiatric history (Schachter & Davis, 2000). The second part is neurological examinations and the third part consists of neuropsychological tests (Bekris et al., 2010).

Different types of brain imaging are often used for early detection of AD, to give a clinical diagnosis. Structural imaging (MRI-magnetic resonance imaging/CT-computed tomography) is used to rule out other types of conditions with similar symptoms which may have treatment options (tumours, brain bleeds, strokes etc). Structural imaging can also be used to detect shrinkage in specific brain regions (for example hippocampus) that are associated with AD. This however is difficult to apply to routine clinical settings (Scheltens et al., 2016).

PET (positron emission tomography) shows how adequately different brain regions function by measuring the use of sugar or oxygen by cells. Fluorodeoxyglucose (FDG) PET scans measure the uptake of glucose by neurons and glial cells and is very sensitive to synaptic dysfunction. If FDG-PETs scans are normal, neurodegenerative diseases can be excluded from the diagnosis. In case of AD, FDG-PET typically shows reduced use of glucose in multiple different brain regions related to memory and learning, for example the hippocampus and prefrontal cortex. However similar to structural imaging, this method is difficult to apply to diagnostic information about one individual (Scheltens et al., 2016). PET imaging can also be used as a molecular imaging type, where specific cellular and chemical changes are detected by using highly targeted radiotracers. There are a few molecular imaging compounds that have already been approved for clinical use to detect β -amyloid- florbetaben, florbetapir and flutemetamol. Although amyloid plaques are one of the first pathological events for AD, this method cannot be used on its own to diagnose AD, since many people, who do not develop AD can still have amyloid plaques in the brain (Herholz & Ebmeier, 2011). PET imaging can also be used to detect tau in the brain with fluorinated ligands that bind to aggregates of tau with notable accuracy (Scheltens et al., 2016).

To give a definitive diagnosis it is required to conduct a post-mortem evaluation of the brain tissue (Weller & Budson, 2018). To then confirm the diagnosis two histopathological features, need to be present in the brain tissue: amyloid plaques and neurofibrillary tangles. Both of these are often found in normal age-matched controls, but the distribution of the tangles and the density of the plaques is more severe in AD patients (Bekris et al., 2010).

1.3 Treatments

Although the disease does not currently have a cure, there are treatments available that can relieve some symptoms and improve the quality of life for a limited period of time. Currently, there are two classes of pharmacologic therapy indicated for AD patients. Cholinesterase inhibitors, including donepezil, rivastigmine and galantamine, are used for patients with any stage of Alzheimer's disease and memantine is used for people with moderate or severe AD. If these treatments are prescribed at the appropriate time during the course of the illness, they have shown to improve the quality of life for the patient. Nonetheless, these medications do not change the rate of decline or change the course of the illness in any way (Weller & Budson, 2018; Bhattacharya et al., 2014).

Many clinical trials have been conducted in AD patients in attempts to develop more treatments; however, the results have not been very promising. There have been treatments that target the β -amyloid clearance, for example Bard et al., 2000, showed that antibodies used against amyloid were able to cross the blood-brain barrier and trigger microglial cells to clear plaques. However the plaques were not cleared to an extent needed to treat AD (Bard et al., 2000; Shukla et al., 2012). Different clinical trials have tried to decrease the production and aggregation of β -amyloid by using inhibitors and modulators that affect different enzymes involved in the processes. However, no clinical efficacy has been shown with these trials. Furthermore, some inhibitors have even worsened some of the symptoms since the enzymes they inhibit may have other important roles. For example, using β site APP cleaving enzyme inhibitors lowered cognitive function (Shi et al., 2020). There have also been trials for treatments that target the production of phosphorylated tau (leuco-methylthionium bis(hydromethanesulphonate) and tideglusib), but they have not shown efficacy (Gauthier et al., 2020). Thus, treatments that can do more than just lower amyloid or tau are highly sought after.

Recently, curcumin has shown promise as another treatment option for neurodegenerative diseases, including AD, based on the much lower prevalence of dementia in countries consuming high levels of -curcumin, which is a base component of Ayurvedic diet. Curcumin has anti-inflammatory, anti-amyloid and antioxidant properties. Furthermore, curcumin is lipophilic, which allows its absorption. However, it is heavily metabolised, which reduces the amount that gains access to brain (Begum et al., 2008; Hickey et al., 2012). In vitro studies have shown that using curcumin as pre-treatment, in neuroblastoma cells, increases mRNA and protein levels of mitochondrial genes, which prevents β -amyloid induced toxicity (Reddy et al., 2016). In vivo curcumin reduces amyloid and importantly, it decreases levels of inflammatory molecules and therefore suppresses neuroinflammatory responses (Hickey et al., 2012; Begum

et al., 2008). However, curcumin alone reaches minimal levels in brain. Thus, great attention has been paid to protecting curcumin from metabolism and to formulating it to increase its delivery to brain (reviewed by Gagliardi et al., 2020). In particular, several studies have now shown that nanoformulated curcumin increases its delivery to brain in animal models of AD, and these nanoformulations confer greater beneficial effects on cognitive impairment, inflammation and neurodegeneration compared with curcumin alone (Kakkar & Kaur, 2011; Huang et al., 2017; Gao et al., 2020).

Studies of curcumin in AD patients are limited by the fact that two studies which have now been examined showed extensive glucuronidated metabolites indicating extensive metabolism (Ringman et al., 2012; Baum et al., 2008). Thus, research continues to improve curcumin bioavailability to enable this safe compound to be used in AD.

1.4 Pathology in Alzheimer's disease

1.4.1 Gross pathology

In patients with AD there is a loss of neurons and synapses in cortical and subcortical regions of the brain, which leads to degeneration of the affected areas, which can ultimately cause brain shrinkage and an increase in ventricle sizes (see Fig. 2). The regions of the brain that are affected the most in AD are temporal, frontal and parietal lobes, frontal cortex and the hippocampus (Wenk, 2003).

One important pathological event in AD is the loss of forebrain cholinergic neurons (Nyakas et al., 2011), which are nerve cells that provide the cerebral cortex with a primary source of acetylcholine, which plays a critical role in its development and maintenance (Schliebs & Arendt., 2011). Furthermore, acetylcholine is very important in terms of attention and learning (Gauthier, 2002). A decline in the activity of choline acetyltransferase and acetylcholine esterase are common events in AD, which further lead to a decline in acetylcholine release (Nyakas et al., 2011). Current symptomatic treatments (for example Rivastigmine) alleviate this deficit by inhibiting acetylcholine degradation; however, these drugs have no effect on disease progression (Khoury et al., 2018).

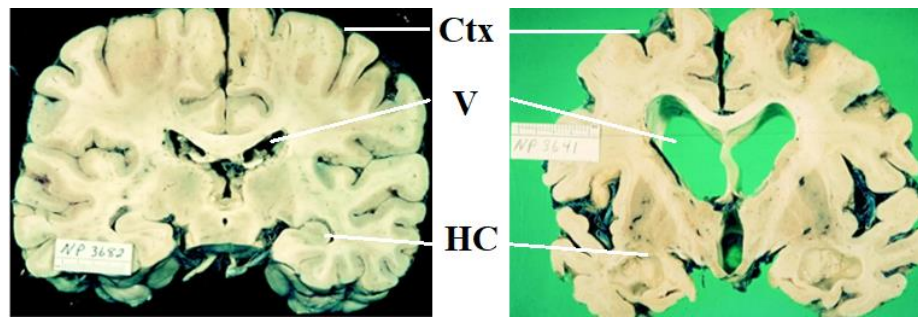


Figure 2. Comparison of a normal human brain and degeneration from severe AD. The folds and grooves of the cerebral cortex (Ctx) are severely decreased, while ventricles (V) are enlarged. There is also shrinkage of the hippocampus (HC) (adapted from Bird, 2008).

1.4.2 Microscopic pathology

1.4.2.1 Amyloid and tau pathology in Alzheimer's disease

Two main neuropathological hallmarks that characterise Alzheimer's disease are the extracellular amyloid plaque that is formed by β -amyloid protein aggregates and intracellular neurofibrillary tangles that are composed of hyperphosphorylated tau proteins (Fig. 3). Both amyloid plaques and neurofibrillary tangles are considered to be involved in the neuronal dysfunction that leads to neuron loss (Serrano-Pozo et al., 2011).

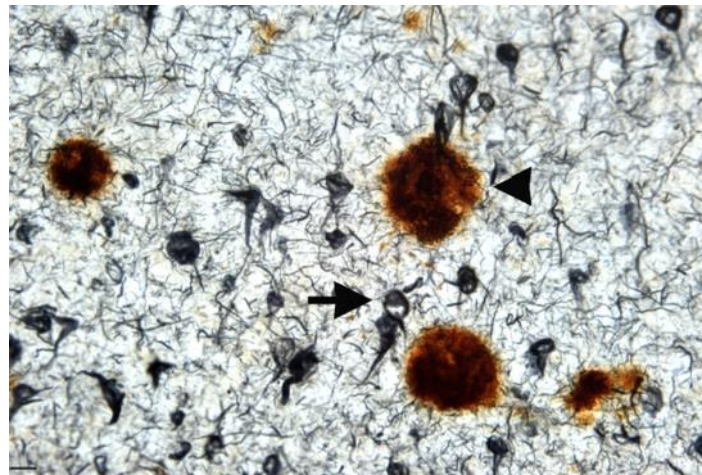


Figure 3. Amyloid plaques and neurofibrillary tangles in AD. Arrowhead shows the accumulation of β -amyloid plaques and the arrow shows the neurofibrillary tangle composed of hyperphosphorylated tau (Adapted from Rohn, 2013).

The β -amyloid protein is formed by the proteolysis of its precursor protein- APP, which is expressed at high levels in the brain. Mutations in the critical regions of the APP gene that codes for the protein can affect its processing and thus the production of β -amyloid (Murphy & LeVine, 2010). The two main enzymes involved in the breakdown of APP to generate β -amyloid are β -secretase and γ -secretase (See Fig. 4). The polypeptides that are formed will be in different lengths (37-49 amino acid residue), depending on the cleavage site on γ -secretase (Chen et al., 2017).

The dominant β -amyloid form found within plaques is the 42-residue form (β -amyloid 42) (Wolfe, 2007). β -amyloid 42 is prone to aggregation (Selkoe, 2001), which is considered toxic. Mutations in presenilins, which form subunits within γ -secretase, cause a higher production rate of β -amyloid 42, which further increases its toxicity due to the higher aggregation potential (Wolfe, 2007). The monomeric forms of disease-associated β -amyloid undergo oligomerization, where they form dimers, tetramers, and etc which are still soluble, however oligomeric forms lose their solubility as the aggregates become larger. The continued accumulation leads to the formation of fibrils with β -sheet-structures, the base components of plaques (Cline et al., 2018).

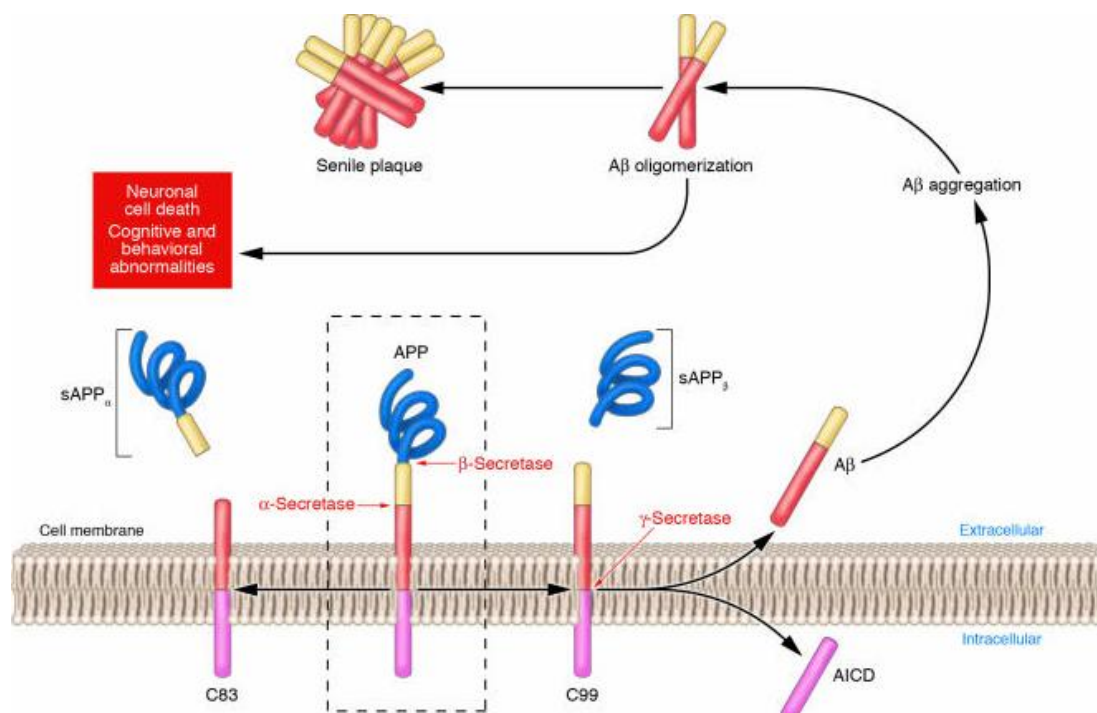


Figure 4. APP processing and the accumulation of β -amyloid. APP (inside the dashed box) is cleaved by α -secretase or β -secretase forming sAPP $_{\alpha}$, C83 (membrane bound C-terminal fragment of 83) and sAPP $_{\beta}$ and C99 (membrane bound C-terminal fragment of 99). C99 is further cleaved by γ -secretase forming AICD (APP intracellular domain) and β -amyloid (A β). A β is then aggregated into smaller multimers (oligomers). Oligomers are neurotoxic while the end-stage senile plaque is rather passive (adapted from Gandy, 2005).

Phosphorylated tau protein normally stabilises axonal microtubules and regulates neurite outgrowth in the central nervous system. However, under certain conditions tau can become hyperphosphorylated, which reduces its affinity to bind to microtubules, leading to intraneuronal accumulation and aggregation of tau. These accumulations in dendrites affect normal neuronal cell communication which leads to further decline in neurodegeneration. In addition to affecting binding, tau hyperphosphorylation also affects its ability to be degraded (Hoover et al., 2010; Rodríguez-Martín et al., 2013).

1.4.2.2 Neuroinflammation in AD

Research suggests that microglial dysfunction plays a central role in the development and progression of neuroinflammation and Alzheimer's disease. Microglial cells are located in the central nervous system and normally act as a form of immune defence by removing damaged neurons and infections. Many studies have shown that reducing microglia function early in AD disease progression is deleterious. In AD, microglia are activated by amyloid (See Fig. 5) and ingest it. However, over time, they become incapable of clearing the toxic amyloid plaques but retain the ability to recruit further immune cells, which leads to further neurodegeneration (Kinney et al., 2018).

Furthermore, when microglia are activated due to pathological impact, it can lead to production of quinolinic acid, an excitotoxin, and altered phagocytic activity (Wendt et al., 2017; Whiley et al., 2021).

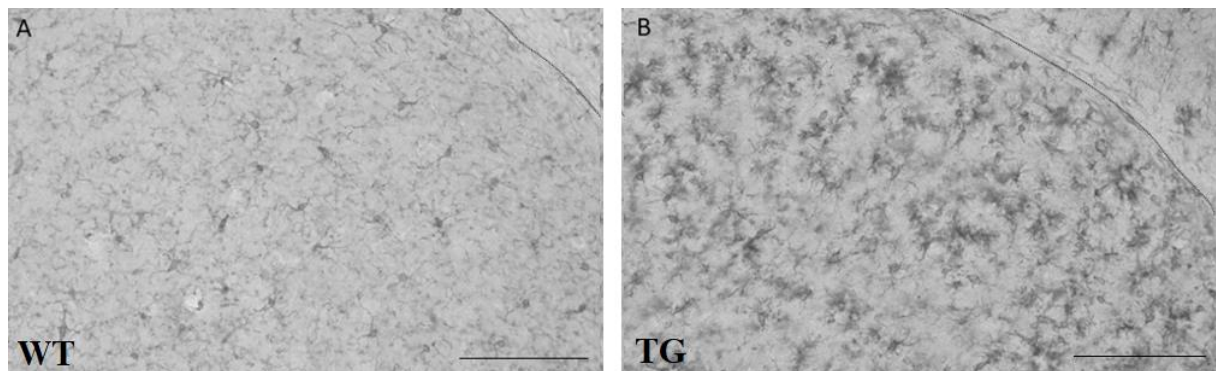


Figure 5. Microglia staining in 6-month-old female mice brain. (A) Wildtype and (B) 5xFAD transgenic mouse sagittal sections of the brain stained with IBA1 antibody. Subiculum region, approximately 2.6 mm lateral of Bregma is shown. Note that in addition to an increased number of microglia, the morphology of microglia changed dramatically in comparison to the WT mouse. The dashed line shows the border of the subiculum with the corpus callosum. Scale bar, 100 μ m, for both photomicrographs.

1.5 Transgenic mouse models of Alzheimer's disease

1.5.1 Overview of mouse models

A lot of the AD transgenic mouse models are based on the overexpression of mutant forms of APP (amyloid precursor protein), tau, or presenilins that cause an increase in the production of β -amyloid and its accumulation into plaques or tau into neurofibrillary tangles. These transgenes can cause progressive neurodegeneration which can lead to similar behavioural disruptions as seen in human AD patients (Sasaguri et al., 2017). One of the most widely used APP based mouse models is the 5xFAD model.

1.5.2 5xFAD mouse model

This transgenic mouse model for Alzheimer's disease carries 5 mutations that are associated with fAD (familial Alzheimer's disease). There are 3 APP mutations and 2 presenilin (PS1, PS2) mutations (see Fig. 6), which are known to cause an increase in the production of β -amyloid 42 and cleave it incorrectly (Oakley et al., 2006).

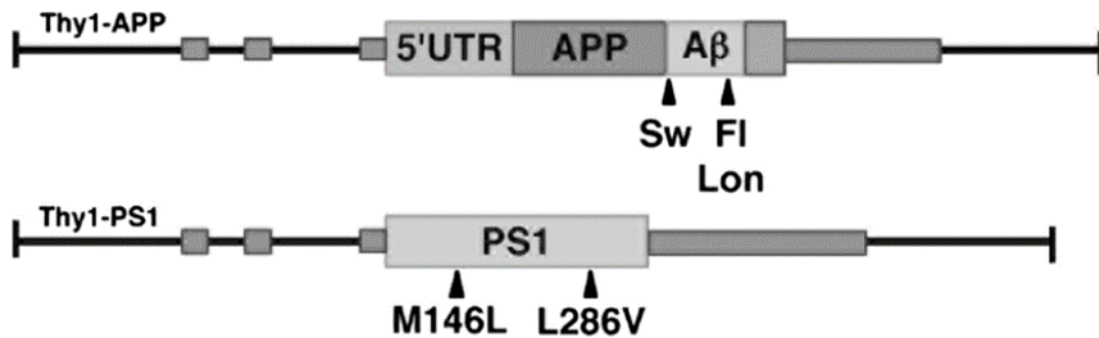


Figure 6. 5xFAD APP and PS1 transgenes. Triangles indicate the FAD mutations in APP and PS1 transgenes expressed under the control of the Thy1 promoter which is expressed predominantly in neurons. Sw-Swedish mutation; FI-FL mutation; Lon-London mutation; M146L-PS1 mutation; L286V-PS1 mutation. Small grey rectangles mark Thy1 exons and the larger rectangles represent the coding regions of APP and PS1 (Adapted from Oakley et al., 2006).

This mouse model is widely used due to the many AD-related phenotypes they recapitulate, and they have a relatively aggressive and early presentation (Oakley et al., 2006).

5xFAD mice also display a range of motor and cognitive deficits. Beginning at the age of 4 to 5 months spatial working memory is impaired. This was tested with spontaneous alternation in the Y-maze by Oakley et al., 2006. This task does not involve any rewards, punishments, or training, which allowed to assess hippocampus-dependent spatial working memory (See Fig. 7). Mice were significantly impaired in this task by the age of 4-5 months compared to wild-type mice (Oakley et al., 2006). However, the group size used in this trial (n=12-20) was rather imbalanced. Indeed, publications using this task in 5xFAD mice show very inconsistent results and poorly described methods and materials (gender not reported (Devi & Ohno, 2010); group size imbalanced (Deyts et al., 2019; Devi et al., 2015); no difference between WT and 5xFAD (Sosna et al., 2018)).

Indeed, the lack of appropriate power calculations to ensure group sizes are appropriate for all endpoints (behavioural and pathological) continues to be a serious issue in AD preclinical research (Egan & Macleod, 2014). Other serious issues include a lack of randomisation and a lack of blinding (Egan et al., 2016; 2015; Chen et al., 2019; Rahman et al., 2020; Zhang et al., 2020). Given that AD is a clinically diagnosed disease, this general lack of robust trial design is more likely to contribute false positives (Egan & Macleod, 2014).

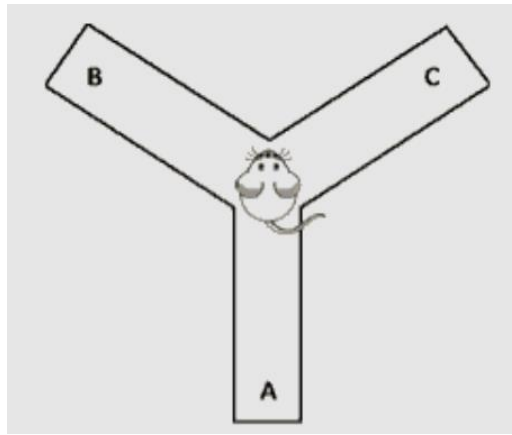


Figure 7. Y-maze test. This test shows the exploring activity of the mouse as rodents normally investigate a new arm in the maze, rather than returning to a previously visited arm. Different brain regions are involved in this task, including the hippocampus and the prefrontal cortex. This test is often used to analyse hippocampus-dependent spatial working memory. Mouse is placed into the central zone of the apparatus. The timer is started, and every one-arm entry is noted. An arm entry is defined as when all four paws have crossed the threshold of the central zone into any of the arms. After the selected time ends, the mouse is removed. As this is thought to mimic foraging behaviour, cognitive impairment is measured as the number of failed trios completed, thus, where the mouse revisits an arm. A successful trio is when the mouse enters 3 different arms in a row (for example: BCA). A failed trio is when the mouse repeats the same arm before entering all 3 arms (for example BCB) (Figure adapted from <https://med.stanford.edu>).

1.5.3 Pathology in 5xFAD mouse model

As discussed above, the 5xFAD mouse model has an early presentation of amyloid plaques in the brain. High levels of intraneuronal β -amyloid 42 have already started accumulating at around 1.5 months of age. At around 2 months of age extracellular amyloid deposition begins, starting first in the subiculum and layer 5 of the frontal, somatosensory cortex. Microgliosis also begins at around 2 months of age. The amyloid deposition increases rapidly with age and by six months of age plaques are present all throughout the layer 5 of the frontal cortex and hippocampus. After 6 months plaques can be found in the thalamus, brainstem, and olfactory bulb. However, plaques are absent from the cerebellum. Female mice exhibit more aggressive plaque pathology than males with higher plaque numbers and density in both the cortex and hippocampus (Oakley et al., 2006). The number on plaques increase gradually until the age of 10 months in males but continues to increase slowly until at least 14 months in females (Bhattacharya et al., 2014).

By 9 months of age significant neuron loss can be seen in cortical layer V and subiculum. Neuron loss occurs in the same regions as the accumulation of intraneuronal β -amyloid 42, which could mean that there is a correlation between the two (Eimer & Vassar, 2013).

In addition to amyloid, this mouse model is also shown to accumulate hyperphosphorylated tau in the hippocampus and cortex. This adds to the age-dependent memory deficits (Shukla et al., 2012). This mouse model shows many human AD-related phenotypes (See Table 2).

Data from other mouse models of AD have clearly shown that inadequate attention to age and endpoint measurement when assessing neuropathology can lead to false positives in preclinical trials. For example, Bexarotene was reported to reduce amyloid in two separate mouse models (APP/PS1 and APPPS1-21 transgenic mice) (Cramer et al., 2012) but more thorough analyses revealed no effects and indeed pointed to variability in amyloid load between mice as a factor in the false positive result (Price et al., 2013; Tesseur et al., 2013). Thus, trial design is an important factor to address for preclinical research.

Table 2. Pathological features of the 5xFAD mouse model compared with patients with AD.

	A β -plaques	Hyperphosphorylated tau	Gliosis	Behavioural deficits	Neuron loss
Human	✓ (van der Kant, et al., 2020)	✓ (van der Kant et al., 2020)	✓ (van der Kant et al., 2020)	✓ (Scheltens et al., 2016)	✓ (Scheltens et al., 2016)
5xFAD	✓ (Oakley et al., 2006)	✓ (Shukla et al., 2012)	✓ (Oakley et al., 2006)	✓ (Oakley et al., 2006)	✓ (Eimer & Vassar, 2013)

1.5.4 Preclinical trials in AD

Although there have been various articles published on guidelines and group sizes for preclinical studies in AD, there is still a lack of randomisation and blinding and poor trial designs with small sample sizes (Gagliardi et al., 2020).

Power analysis may be used to determine the minimum sample size that is required to detect a treatment effect. If the sample size is too small the trial may lead to inconclusive findings and waste time and resources. If the effect size is too small, the relevance of the finding is questionable. Significant overestimation of the sample size may also be a waste of time and resources as the treatment effect may be seen with a smaller sample size (Huang et al., 2017; Shineman et al., 2011; Kieren et al., 2014).

2.EXPERIMENTAL PART

2.1 The aims of the work

Our research group is investigating the effect of nanoformulated curcumin in Alzheimer's disease in 5xFAD mice. In order to determine the best endpoints to use in the preclinical trials, we must first determine appropriate behavioural endpoints, group sizes required and effect sizes, which, is a novel research point in preclinical AD research.

The specific objectives of this study are:

1. To determine whether percent area and particle analysis, based upon IBA1 antibody immunohistochemistry, are appropriate endpoints to use in preclinical trials in young 5xFAD mice.
2. To determine whether cognitive testing using Y maze is a suitable endpoint for use in preclinical trials in young 5xFAD mice.
3. If either endpoint is suitable: To determine appropriate group sizes for use in preclinical trials in young 5xFAD mice and the associated power to detect specific treatment effects.
4. If either endpoint is suitable: based upon the above aims, to examine these endpoints in a preclinical trial of nanoformulated curcumin in 5xFAD mice.

2.2 Materials and methods

2.2.1 Animals

For this work, female 5XFAD and their WT littermates were used as the pathology is more severe in females (MMRRC stock number #34840; background: B6SJLF1) (Oakley et al., 2006). For Aim 1 (pilot neuropathological analysis), a series of mice at 2, 4 and 6 months of age were analysed (N=3-4 female wildtype and transgenic littermates per age). For Aim 2 (pilot Y maze analysis), 4-month-old mice (N=8 WT; N=11 TG) were analysed. For Aim 4 (preclinical trial), mice were treated with nanoformulated curcumin (TG, N=11) or saline (TG, N=10, WT N=14) from 2-4 months of age and then euthanised for neuropathological analysis. All mice were kept under standard laboratory conditions with free access to food and water and on a 12-hour light and dark cycle.

All experiments with animals were performed in accordance with the EU Directive 2010/63/EU and were approved by the Estonian Ministry of Rural Affairs (licences 140 and 175). The mice were handled by Dr MA Hickey who is authorised to perform this work.

2.2.2 Behavioural analysis

For Aim 2 (pilot Y maze analysis), female mice were tested and videotaped by MA Hickey, who is licenced to perform animal experiments, while I assisted. Mice were tested at approximately 4 months of age. After the experiments were finished, I conducted the video analysis. For 30 minutes before testing, the mice were habituated in the testing room. Spontaneous alternation tests were conducted using a Y-maze. Each mouse was placed in the central zone and analysed for 5 minutes and their movement was noted. The criterion for one arm entry was all four paws entering the arm. 70% ethanol was used to clean the maze between trials, which was thoroughly dried before the mouse entered the maze. Experiments were conducted and analysed blind with respect to the genotype of the mice. Percentage alternation was calculated as follows: number of successful triads divided by the maximum possible alternations (total number of entries minus 2) x 100. External cues were provided to enable orientation (see Fig. 7, 8). Experimenter positions, equipment positions and cues were strictly controlled and comparable between trials to ensure consistency. $\frac{\text{Successful triads}}{\text{Possible alternations}} \times 100$



Figure 8. Y-maze test. Set up on the ground with pictures as external cues at each arm.

2.2.3 IBA1 antibody immunostaining for the pilot trial

To generate cryosections for Aim 1 (pilot neuropathological analysis) and Aim 4 (preclinical trial): Following cervical dislocation, the brains of the mice were rapidly dissected. For immunohistochemical studies, one hemisphere was placed in fresh 4% paraformaldehyde overnight at 4°C. Following cryoprotection in 30% sucrose, hemispheres were frozen in liquid nitrogen and stored at -80°C. Sagittal sections (40µm) were taken and stored in cryoprotectant at -20 °C until use.

Aim 1 (pilot neuropathological analysis): For the immunostaining, 2 sections at approximately 2.6mm lateral of Bregma (lateral; frontal cortex and subiculum assessed) and 2 sections at approximately 1.5mm lateral of Bregma (medial; frontal cortex only) were picked from each

mouse. Aim 4 (preclinical trial): 2 sections at approximately 3mm lateral of Bregma were picked from each mouse.

Aims 1 and 4: The sections were washed 3×5 minutes in 0.01M phosphate-buffered saline (PBS). Endogenous peroxidases were then blocked by incubating in 1% H_2O_2 and 0.5% Triton X-100 in PBS, for 20 minutes. Non-specific binding sites were then blocked by incubating at room temperature for 30 minutes in 0.01M PBS containing 5% donkey serum and 0.5% TX-100. Primary antibody (goat polyclonal to IBA1 Anti-IBA1 antibody-ab5076, Abcam) (See Table 3), was diluted (1:1000) in block. 300 μ l was added to microcentrifuge tubes and sections were added. One tube contained only sections and a block as a “no primary” control. Sections were then incubated overnight at room temperature on a moving rack. The following day the sections were washed 3×5 minutes in PBS containing 0.5% TX at room temperature. Then they were incubated in biotinylated donkey anti-goat antibody (1:200, 705-065-147 Jackson ImmunoResearch) (See Table 3) for 2 hours at room temperature. Sections were washed again (3×5 minutes in PBS with 0.5% TX 5min) and then reacted with avidin-biotin complex in PBS containing 0.2% Triton X-100 for 2 hours (2 drops of Reagent A to 5ml of PBS 0.01M + 2 drops of Reagent B to the same container, vortex immediately; Vectastain Elite ABC-HRP Kit, Vecotor labs). Sections were washed again with PBS. Immunoreactivity was visualized by incubation in 0.03% 3-3diaminobenzidine (DAB) tetrahydrochloride and 0.0006% H_2O_2 in 0.05M TB, pH 7.6 (H_2O_2 was added just before development). Sections were washed 3 times in 0.01M TB for 5 minutes and then dehydrated, defatted and mounted on glass slides with mounting medium (Eukitt). No staining was noted in control sections (no primary antibody). Pictures were taken with cellSens Entry, V2.2 software (Olympus Life Science, Center Valley, Pennsylvania). To ensure consistency, all pictures were taken at the same settings, using 20x magnification. Fluorescence staining was also tried with several different concentrations, however there was too much background for a successful analysis.

Table 3. Antibodies used for immunostaining.

	Catalogue no.	Host	Provider	Final dilution
Primary Antibody				
Anti-IBA1	ab5076	Goat	Abcam	1:1000
Secondary Antibody				
Donkey Anti-Goat	705-065-147	Donkey	Jackson ImmunoResearch	1:200

2.2.4 Preclinical trial

The preclinical trial was conducted in the Hickey laboratory, and I performed the analysis on the percent area and particle analysis. In the preclinical trial the effect of nanoformulated curcumin in AD is tested.

Our collaborators have developed a protocol for encapsulating curcumin within H-ferritin nanocages that increases the water solubility of curcumin by 700-fold as curcumin is insoluble in water (Pandolfi et al., 2017). These H-ferritin nanoparticles have been shown to cross endothelium cells in vitro (Shahryari et al., 2016). H-ferritin nanoparticles interact with the transferrin receptor, which is highly expressed on the luminal surface of endothelial cells and are taken up by the blood brain barrier by transcytosis (Li et al., 2010).

2.2.4.1 Brief protocol of preclinical trial

I provide a brief outline of the preclinical trial here but as these data are described elsewhere, no data will be included in this thesis except for IBA1 immunohistochemistry, which I analysed. At 2 months of age, mice were tested for spontaneous activity. Between 2-4 months of age, the mice were treated twice weekly with 1mg/kg curcumin (nanoformulation was diluted in sterile saline for injection) via intraperitoneal injections and their weight recorded. At 4 months of age, mice were tested for spontaneous activity and cognitive performance in the Morris water maze and tissue taken for analysis. Final group sizes are shown in Table 4. Additional mice that were not analysed included one WT and one TG saline-treated mouse that lost weight and that were euthanised early; N=4 mice that did not demonstrate sufficient visual activity for Morris water maze and N=1 mouse where the genotype did not match the original.

Table 4. Mice group sizes for the preclinical trial.

Groups	Final group sizes
WT saline	N=14
TG saline	N=10
TG NFcur (nanoformulated curcumin)	N=11

The mice were recruited in a staggered manner, and TG mice were assigned to treatment groups in a pseudorandomised manner using littermates as controls. Drug administration was not blinded; however, all behavioural testing was conducted blinded and was analysed using computer software (Ethovision, V11). Percent area and particle analysis were also conducted blinded.

2.2.5 Analysis of percent area using ImageJ

IBA1 antibody-stained microglia were analysed using ImageJ 1.53i (W. Rasband, USA, version 1.8.0_172). Percentage area covered by IBA1 staining was measured. Images were changed to 8bit B&W. The threshold (See Fig. 9) was set common to age (2 months-130; 4 months-145; 6 months-150) for Aim 2, as the different ages were developed in DAB separately. A threshold of 135 was common to all for the preclinical trial (Aim 4), as all samples were developed

together. However, due to some variability in background for a small minority of images, threshold was changed for specific pictures. All of the analysis was conducted by myself blinded to genotype to avoid bias.

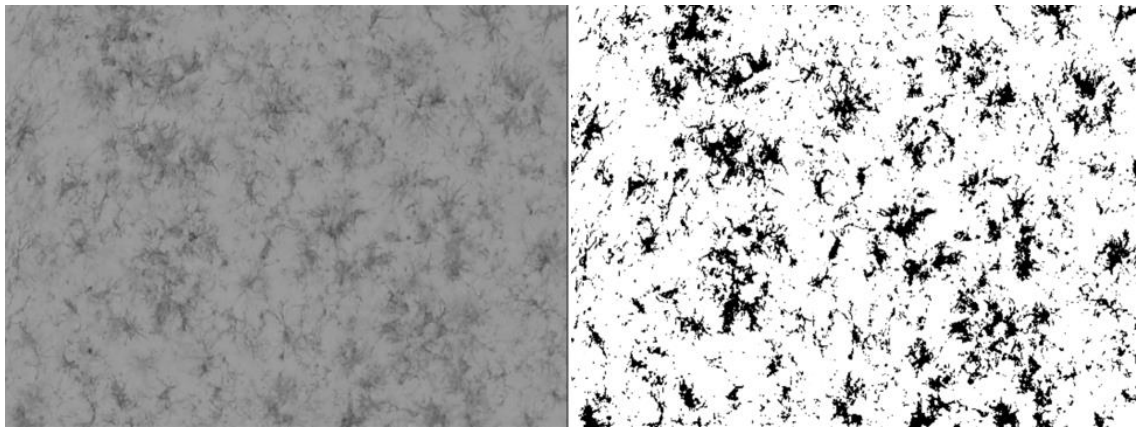


Figure 9. Original (left) vs thresholded image (right) from IBA1 immunostaining from the pilot trial at 4 months. Image taken at 20x in the subiculum. Threshold was set to 145.

2.2.6 Particle analysis using ImageJ

IBA1 antibody-stained microglia were analysed using ImageJ 1.53i (W. Rasband, USA, version 1.8.0_172). Images were processed as for the skeleton analysis (Young & Morrison, 2018). All processing was automated to remove bias, but the process was checked to ensure processing was faithful to original images. Images were FFT bandpass filtered, converted to grayscale, brightness and contrast were adjusted automatically, then an unsharp mask was run twice, images were then despeckled, and converted to binary using the RenyiEntry for automated thresholding. The final images were then despeckled, and the close and remove outliers' plugins were used to close objects and smooth final objects. All particles greater than $30\mu\text{m}^2$ were measured (See Fig. 10). The analysis was conducted blinded to genotype and treatment.

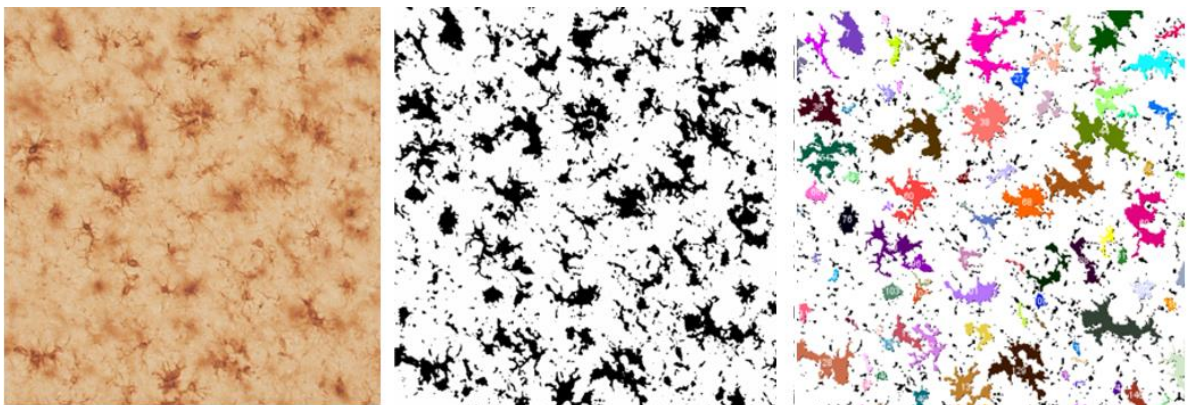


Figure 10. Particle analysis from IBA1 immunostaining from the pilot trial at 4m. Image taken at 20x in the frontal cortex. All particles larger than $30\mu\text{m}^2$ are measured (marked with colour and number) on the right.

2.2.7 Statistics

Mean values \pm standard error of the mean (SEM) was used to present the data. The critical value was set to 0.05. Šidak's multiple comparisons test, Tukey's multiple comparisons test and ANOVA tests (1-way and 2-way) were used for the analysis. This was done to avoid type I error, which gives a false positive. For power analysis ClinCalc was used to determine the minimum number of subjects for adequate study power (Kane, 2019).

2.3 Results and discussion

2.3.1 Behavioural analysis

Working memory of 5xFAD female transgenic and wild-type (WT) littermates was assessed based upon spontaneous alternation in the Y-maze (4m old; N=11 TG, N=8 WT).

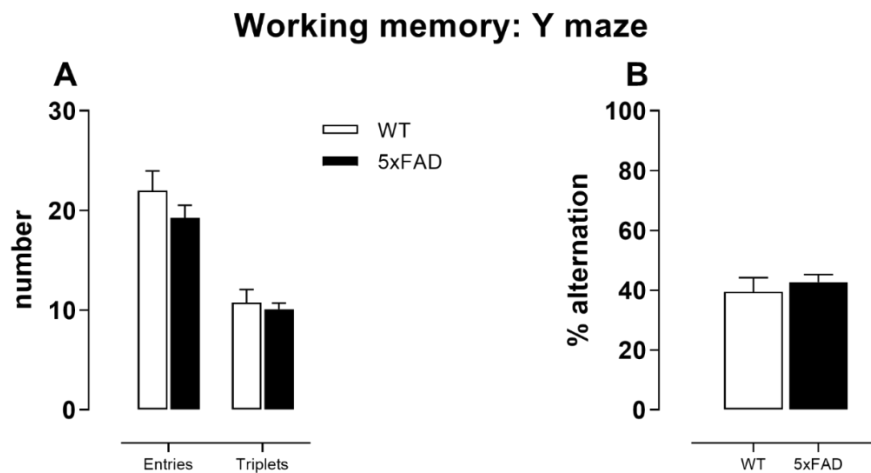


Figure 11. Y-maze test results. N= 11TG, 8WT (A) Activity levels, assessed by number of entries and number of triplets completed within 5 minutes. No difference in baseline activities was detected in 5xFAD transgenic mice. (B) The percent alternation was not significantly different between the genotypes, demonstrating that this test is not a robust endpoint to use for cognition in 5xFAD transgenic mice at this age.

Both genotypes gave very similar results for the Y-maze testing (See Fig. 11). There was no significant difference in the number of entries or successful triplets between the WT and TG mice ($p>0.05$). Furthermore, there was no significant difference between the TG and WT mice in percent alternation ($p>0.05$).

This finding has been repeated in the Hickey laboratory in a larger group of mice- females; 4-5m old; N=14WT, 16TG. Moreover, aging the mice did not reveal any impairment because motor activity declines, precluding the ability to detect differences.

The Y maze test has been used by many people; however, the results seem to be inconsistent and unreliable (Table 5).

Table 5. Previous publications using the Y-maze to test cognition in 5xFAD mice.

Paper	Group size	Age	Gender	Test length	Effect (size)
Original paper (Oakley et al., 2006)	12-21	4m	?	8min	↓ (-10%)
(Devi & Ohno, 2015)	11-13	4m	?	8min	None
(Pagnier et al., 2018)	5	5m	Males	?	↓ (≈-20%)
(Sosna et al., 2018)	4-12	5m	M+f	8min	None
(Deyts et al., 2019)	6-25	5-6m	?	up to 10min	↓ (≈-8%)
(Devi & Ohno, 2010)	5-12	6m	?	8min	↓ (≈-10%)
(Shukla et al., 2012)	>12	6m	M+f	8min	↓ (≈-20%)
(Devi et al., 2015)	7-18	6m	M+f	8min	↓ (≈-8%)
(Kang et al., 2018)	10	6m	Male	8min	↓ (≈-25%)
(Yang et al., 2018)	9-12	6m	?	8min	↓ (≈-40%)

We note that we used 5 minutes for testing, as used by others (Wolf et al., 2016; Cleal et al., 2021). This reduction in testing time is unlikely to have resulted in an inability to detect cognitive deficits but may have reduced the number of entries made. This suggests the significant impact of spontaneous motor function on the test. Towards this end, cognitive tests that use, e.g., swimming, are immune to such issues of motivation (Vorhees & Williams, 2006). Moreover, other issues with this task include the fact that high triplet scores suggest stereotyped behaviour (Cleal et al., 2021).

In conclusion, since this endpoint is not suitable for this preclinical trial in young 5xFAD mice, analysis for finding appropriate group sizes was not conducted and this analysis was not used for the preclinical trial. Another behavioural endpoint should be used for the preclinical trial, that shows a difference between the genotypes. For example, Morris water maze has been used in the Hickey laboratory, where there was a difference between genotypes, although it was subtle at 4 months.

2.3.2 Percent area based upon IBA1 immunostaining

Percent area has been used by many researchers for analysis of microgliosis in mice (Song et al., 2018). However, we are unaware of previous efforts to determine appropriate group sizes (Huang et al., 2017; Kieren et al., 2014; Shineman et al., 2011). Many authors have also proposed analysis of morphology of microglia as the morphology changes dramatically with age in 5xFAD mice (see Fig. 5, Fig. 12). However, analysis of morphology is far more labour intensive (Young & Morrison, 2018). We therefore elected to use percent area covered by IBA1 positivity to enable more efficient analysis. Percent area covered by IBA1 positivity captures morphological change and increased number of microglia.

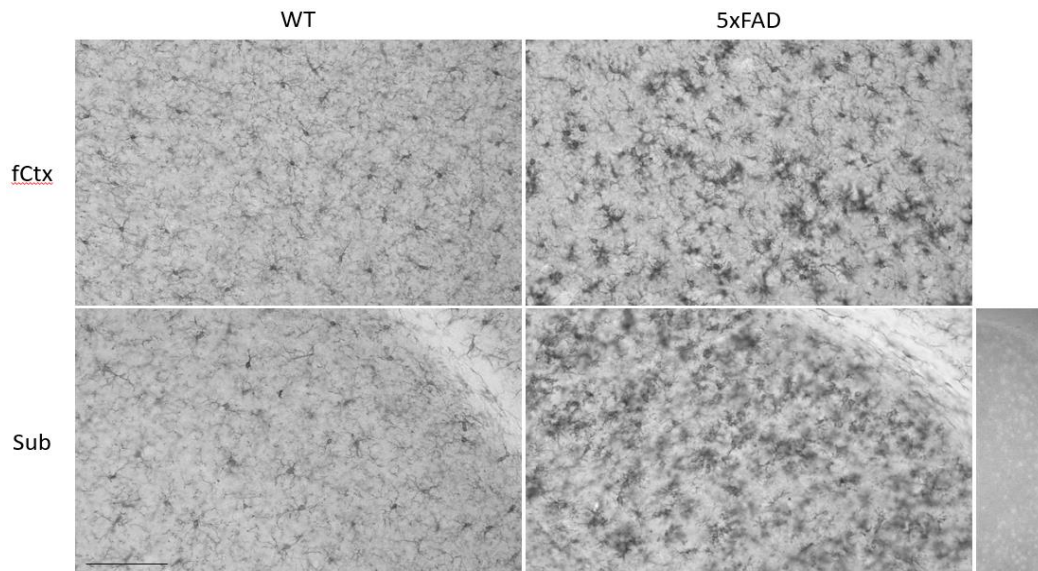


Figure 12. IBA1 immunostaining from the pilot trial at 4m (Aim 1). Morphology of microglial cells in the subiculum (Sub) and frontal cortex (fCtx) in WT and 5xFAD mice. Images were taken at 20x and the scalebar is 100 μ m. The low-power (x10) image on the lower right shows no primary control.

For the pilot trial (Aim 1), IBA1 antibody immunostaining was performed and analysed on female 5xFAD transgenic (TG) and WT littermates. Mice were 2 (N=3WT, 3TG), 4 (N=3WT, 3TG) and 6 months (n=3WT, 4TG) old to determine the progression of microgliosis with age with respect to percent area. Since immunostaining was completed separately for each age group, the results were compared within age.

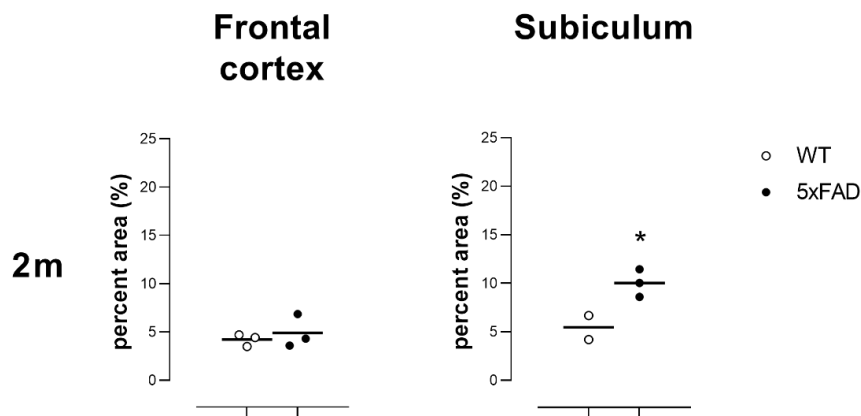


Figure 13. Percent area at 2 months with IBA1 immunostaining. N=3WT,3TG. Area calculated with ImageJ. Percent area in 2m old 5xFAD and their WT littermates in frontal cortex (medial + lateral) and subiculum (lateral only, data from one WT mouse lost due to damage to cryosections). No significant increase in percent area was observed in the frontal cortex in 2-month 5xFAD mice compared to WT. There is a small difference in microglial percent area in the subiculum. Lines depict means. * p<0.05

At 2m of age (See Fig. 13), there was a significant effect of region, meaning that overall, percent area in the subiculum is different to the frontal cortex ($F(1,7) = 13.45$ p<0.01). There was also a significant overall effect of genotype, meaning that transgenic mice were different from WT mice overall ($F(1,7) = 9.454$ p<0.05). Šídák's multiple comparisons tests revealed a weak

significant difference between transgenics and WT mice within the subiculum at this age ($p < 0.05$). These data are in keeping with the early appearance of microgliosis and neuropathology in these mice (Oakley et al., 2006).

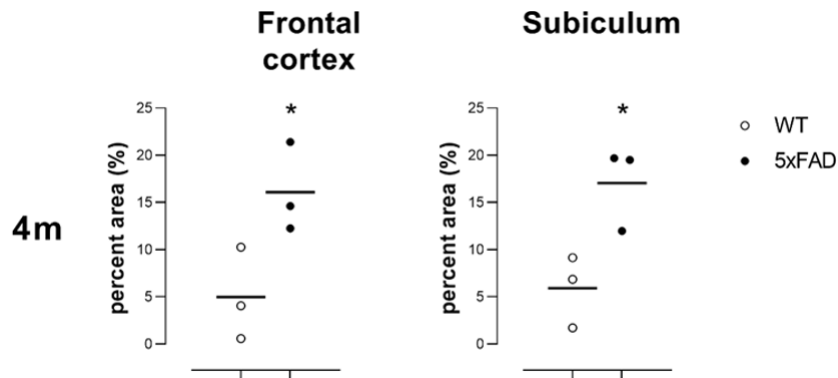


Figure 14. Percent area at 4 months of age with IBA1 immunostaining. N=3WT,3TG. Percent area calculated with ImageJ. Percent area in 4m old female 5xFAD and their WT littermates in frontal cortex (medial + lateral) and subiculum (lateral only). There is a significant increase in percent area in both the frontal cortex and in the subiculum in 4-month 5xFAD mice compared to WT. However, there is also significant variability within groups. Lines depict means. * $p < 0.05$

At 4m of age (See Fig. 14), there was a significant effect on genotype ($F(1,4) = 19.85, p < 0.05$), which means that the percent area in mutant mice is significantly different to the percent area in WT mice, overall. There was no significant difference in region ($F(1,4) = 0.1297, ns$). Šídák's multiple comparisons tests revealed a weak significant difference between mutants and WT mice in both subiculum and frontal cortex ($p < 0.05$). However, the data are variable, which means that this endpoint is used in a preclinical trial, sufficient mice must be included to avoid Type I (false positive) or Type II errors (false negative).

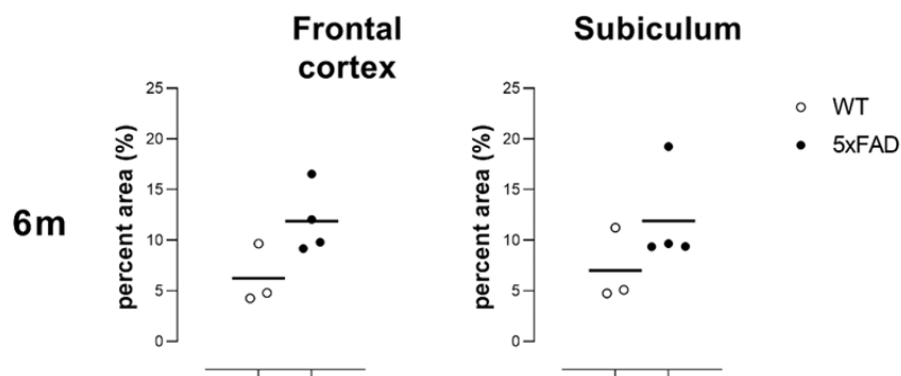


Figure 15. Percent area at 6 months with IBA1 immunostaining. N=3WT,4TG. Percent area calculated with ImageJ. Percent area in 6m old female 5xFAD and their WT littermates in frontal cortex (medial + lateral) and subiculum (lateral only). There is a significant increase in percent area in the frontal cortex and in the subiculum in 5xFAD mice compared to WT. Lines depict means.

There is a significant overall effect on genotype, at 6m of age (See Fig. 15), ($F(1,5) = 7.042, p < 0.05$), which means that the percent area in mutant mice is significantly different to the percent area in WT. However, the significance is smaller than for 4-month-old mice, which

may be due to an increase in baseline in WT mice as a factor of age, as has been shown for astrocytes in WT mice (Hickey et al., 2008).

2.3.2.1 Power analysis of percent area

Power analysis was used to determine the appropriate sample size to detect a treatment effect for a preclinical trial (See Table 6,7). To enable sufficient time to treat adult mice, the earliest endpoint possible was 4m (mice do not become sexually mature until approximately 6 weeks of age; thus, 2m is too early as an endpoint). ClinCalc sample size calculator was used with two independent study groups design and a continuous endpoint. The mean and standard deviation of the TG group at 4m was used to determine group sizes required for a reduction to WT levels at 4m or a reduction of 50% or 30% at 4m.

Table 6. Power analysis of percent area in subiculum at 4m.

Group	To bring to WT levels	To reduce by 50%	To reduce by 30%
Sample Size			
TGs at 4m	2	4	13
“Treated” TGs at 4m	2	4	13
Total	4	8	26
Data	IBA1 % area	IBA1 % area	IBA1 % area
Study Parameters			
Mean, TGs at 4m	17.06	17.06	17.06
Mean, “Treated” TGs at 4m	5.921	8.05	12.03
Alpha	0.05	0.05	0.05
Beta	0.2	0.2	0.2
Power	0.8	0.8	0.8

Alpha is the probability of a type I error (false positive), meaning the likelihood of determining a difference where there is none. Beta is type II error, meaning the likelihood of missing a difference (false negative). Power is the likelihood of detecting a difference, if present.

From the power analysis of subiculum data (See Table 6), we have an 80% likelihood (power) of observing a 50% reduction if we have 4 mice in each group and seeing a 30% reduction if we have 13 mice in each group. This is because in order to see a smaller reduction there needs to be more mice in each group due to the variability within the group.

Table 7. Power analysis of percent area in frontal cortex (medial + lateral) at 4m

Group	To bring to WT levels	To reduce by 50%	To reduce by 30%
Sample Size			
TGs at 4m	3	5	15
“Treated” TGs at 4m	3	5	15
Total	6	10	30
Data	IBA1 % area	IBA1 % area	IBA1 % area
Study Parameters			
Mean, TGs at 4m	16.0978333	16.0978333	16.0978333
“Treated” TGs at 4m	5	8	11.3
Alpha	0.05	0.05	0.05
Beta	0.2	0.2	0.2
Power	0.8	0.8	0.8

Alpha is the probability of a type I error (false positive), meaning the likelihood of determining a difference, where there is none. Beta is type II error, meaning the likelihood of missing a difference (false negative). Power is the ability to detect a difference, if present.

From the power analysis of the frontal cortex (See Table 7), we can see that we have an 80% likelihood of detecting a 30% reduction if we have 15 mice in both groups and 5 mice in each group would be required to detect a 50% reduction.

2.3.3 Particle analysis based upon IBA1 antibody immunostaining

When analysing percent area there was variability in the results which could affect the preclinical trial, thus another method for analysing microglia was tested. Area covered by IBA1 antibody staining was analysed by measuring all particles larger than $30\mu\text{m}^2$. Therefore, the analysis “caught” the soma and missed the small processes from the background, that were otherwise counted with percent analysis. This measurement therefore provides a simple and efficient method of measuring extent of microglial arborisation. As previously, the results were compared within age (See Fig. 16).

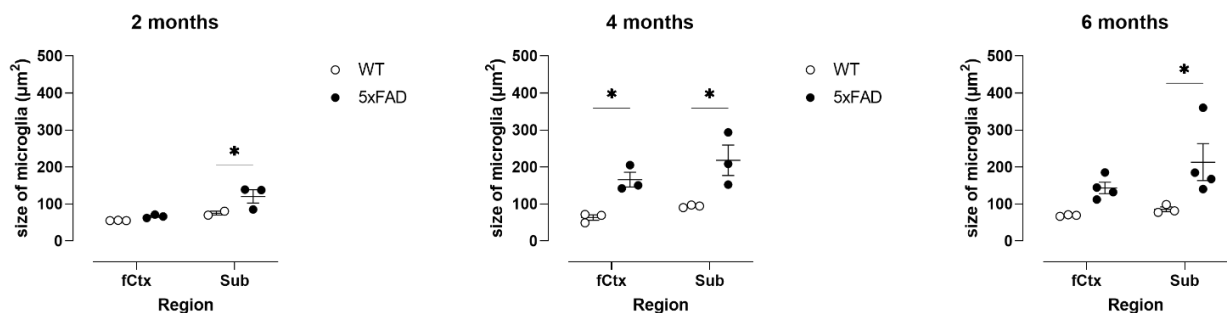


Figure 16. Microglial size with IBA1 immunostaining. Size was calculated with ImageJ. Microglial size in 2- (N=3WT,3TG), 4-(N=3WT,3TG), 6-month-old (N=3WT,4TG) female 5xFAD and their WT littermates in frontal cortex (medial + lateral; fCtx) and subiculum (lateral only; Sub). Data from 1 WT mouse lost due to damage). Lines depict means with SEM.

At 2m of age, there was no significant overall effect of genotype on microglial size (See Fig. 16), meaning that transgenics were not different from WT mice overall ($F(1,4) = 7.340$, ns).

There was a significant effect of region, meaning that overall, microglial size in the subiculum is different to the frontal cortex ($F(1,3) = 12.91$, $p < 0.05$). Šídák's multiple comparisons tests revealed a weak significant difference between transgenics and WT within the subiculum ($p < 0.05$).

At 4m of age (See Fig. 16), there was a significant effect on genotype ($F(1,4) = 14.56$, $p < 0.05$), which means that the microglial size in mutant mice is significantly different to the microglial size in WT, overall. There was also a significant difference in region ($F(1,4) = 0.9.438$, $p < 0.05$). Šídák's multiple comparisons tests also revealed a weak significant difference between mutants and WT in both subiculum and frontal cortex ($p < 0.05$). However, the data are variable in TG mice, especially in the subiculum, which means that when this endpoint is used in a preclinical trial, an adequate number of mice must be included to avoid false positives or negatives.

At 6m of age (See Fig. 16), there is a significant overall effect on genotype ($F(1,5) = 13.86$, $p < 0.05$), which means that the microglial size in mutant mice is significantly different to the microglial size in WT. However, the data is even more variable in TG mice as the disease has progressed noticeably. Šídák's multiple comparisons tests revealed a weak significant difference between transgenics and WT within the subiculum ($p < 0.05$).

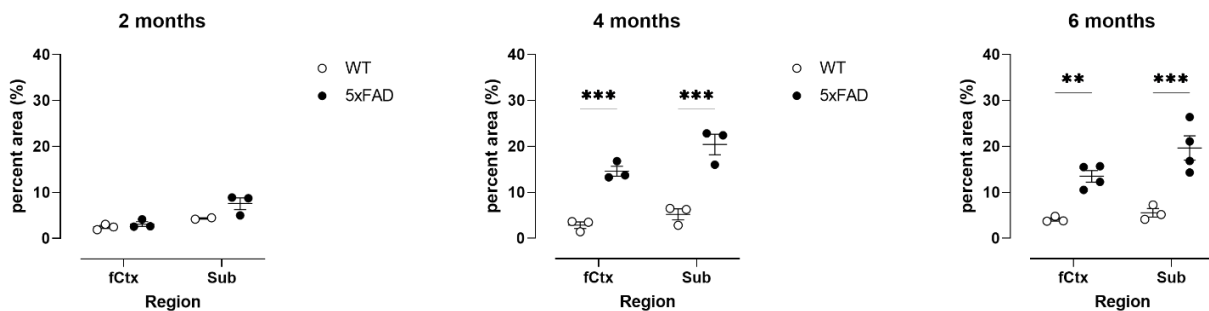


Figure 17. Percent area containing IBA1 immunostaining of greater than $30\mu\text{m}^2$. Percent area was calculated with ImageJ in 2-($N=3\text{WT},3\text{TG}$), 4-($N=3\text{WT},3\text{TG}$), 6-month-old ($N=3\text{WT},4\text{TG}$) female 5xFAD and their WT littermates in frontal cortex (medial + lateral, fCtx) and subiculum (lateral only, Sub). Data from 1 WT mouse lost due to damage. Lines depict means \pm SEM.

At 2m of age (See Fig. 17), there was no significant difference of genotype ($F(1,4) = 4.217$, ns). There was however a significant effect in region, ($F(1,3) = 23.19$, $p < 0.05$).

At 4m of age (See Fig. 17), there was a strong significant overall effect on genotype ($F(1,4) = 56.44$, $p < 0.01$) and a significant overall effect in region ($F(1,4) = 20.90$, $p < 0.05$). Šídák's multiple comparisons tests revealed a strong significant difference between transgenics and WT within both subiculum and frontal cortex ($p < 0.001$).

At 6m of age (See Fig. 17), there is a very strong significant overall effect on genotype ($F(1,5) = 97.52, p < 0.001$), which means that the percent area containing microglia is very different in mutant mice compared to WT. There was no significant difference in region ($F(1,5) = 2.935, ns$). However, the data from the TG mice is more variable than at 4 months of age. Šídák's multiple comparisons tests revealed a strong significant difference between transgenics and WTs within the subiculum ($p < 0.001$) and within the frontal cortex ($p < 0.01$).

2.3.3.1 Power analysis based on the results of the particle analysis

Power analysis was once again used to determine the appropriate group sizes to detect a treatment effect for the preclinical trial (See Table 8, 9). ClinCalc sample size calculator was used with two independent study groups design and a continuous endpoint. To determine sample sizes required for a reduction to WT levels or a reduction of 50%, 30% or 20% at 4m, the mean and standard deviation of the TG group (percent area containing microglia larger than 30 μ m lateral and medial) at 4m was used.

Table 8. Power analysis of percent area containing microglia in subiculum at 4m.

Group	To bring to WT levels	To reduce by 50%	To reduce by 30%
Sample Size			
TGs at 4m	1	2	3
"Treated" TGs at 4m	1	2	3
Total	2	3	12
Data	IBA1 % area	IBA1 % area	IBA1 % area
Study Parameters			
Mean, TGs at 4m	20.42	20.42	20.42
Mean, "Treated" TGs at 4m	5.218	10.21	14.294
Alpha	0.05	0.05	0.05
Beta	0.2	0.2	0.2
Power	0.8	0.8	0.8

Alpha is the probability of a type I error (false positive), meaning the likelihood of determining a difference where there is none. Beta is type II error, meaning the likelihood of missing a difference (false negative). Power is the likelihood of detecting a difference, if present.

From the power analysis of the subiculum data (See Table 8), we have an 80% likelihood (power) of observing a 50% reduction if we have 2 mice in each group and seeing a 30% reduction if we have 3 mice in each group. This analysis shows that particle analysis is a good endpoint to use as to see treatment effect not a lot of mice are needed. However, these sample sizes are really small and not very reliable to use in a preclinical trial and more mice should definitely be included to avoid obtaining insignificant results.

Table 9. Power analysis of percent area containing microglia in frontal cortex at 4m.

Group	To bring to WT levels	To reduce by 50%	To reduce by 30%
Sample Size			
TGs at 4m	0	1	3
“Treated” TGs at 4m	0	1	3
Total	0	2	6
Data	IBA1 % area	IBA1 % area	IBA1 % area
Study Parameters			
Mean, TGs at 4m	14.596	14.596	14.596
“Treated” TGs at 4m	2.863	7.298	10.2172
Alpha	0.05	0.05	0.05
Beta	0.2	0.2	0.2
Power	0.8	0.8	0.8

Alpha is the probability of a type I error (false positive), meaning the likelihood of determining a difference where there is none. Beta is type II error, meaning the likelihood of missing a difference (false negative). Power is the likelihood of detecting a difference, if present.

From the power analysis of the frontal cortex (See Table 9), we can see that we have an 80% likelihood of detecting a 30% reduction if we have 3 mice in both groups and 7 mice in each group would be required to detect a 20% reduction. These group sizes are again really small and for the preclinical trial more mice should be included to avoid unfair results.

In conclusion, the best endpoint to use, in the preclinical trial, based on these tests is the particle analysis of percent area covered by microglia and microglia size. These results were the least variable and showed a clear and significant difference between WT and TG mice. The results from the Y-maze did not show any significant differences between WT and TG. The percent area showed a significant effect between WT and TG; however, the results were more variable than with particle analysis.

2.4 Preclinical trial

2.4.1 Percent area from the preclinical trial

For the preclinical trial (Aim 4), IBA1 antibody immunostaining was performed and analysed on female 5xFAD transgenic untreated mice and 5xFAD transgenic mice, treated with nanoformulated curcumin and WT littermates. The mice were 4 (N= 14WT saline, 10TG saline, 11TG NFcur) months old (See Fig. 18).

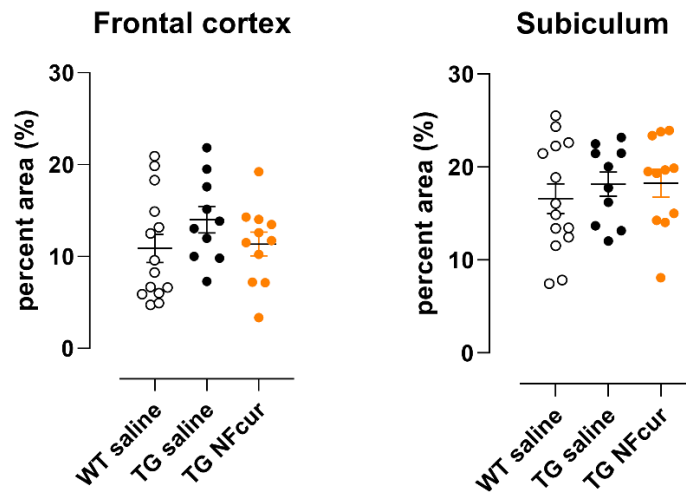


Figure 18. Percent area with IBA1 immunostaining. N=14WT saline,10TG saline,11TG NFcur. Percent area calculated with ImageJ. Percent area in 4-month-old female 5xFAD treated with nanoformulated curcumin (TG NFcur) compared with control TG and WT mice, who were treated with saline in frontal cortex and subiculum. Lines depict means \pm sem.

Using this method, no difference in percent area was detected in treated TG mice compared to WT and untreated TG mice in both frontal cortex and subiculum (there was an overall effect of region ($F(1,32) = 48.78, p < 0.0001$)). This can be due to morphology of the microglial cells being very different (Fig. 19) and the inability of the analysis method to sufficiently capture these differences in morphology. For example, resting microglia are ramified and typically non-overlapping, as we observed in the WT mice here (Torres-Platas et al., 2014). However, microglia in the TG mice were extremely highly ramified and overlapped. Due to this reason, capturing morphology seems to be a more appropriate endpoint to see results from microglial analysis.

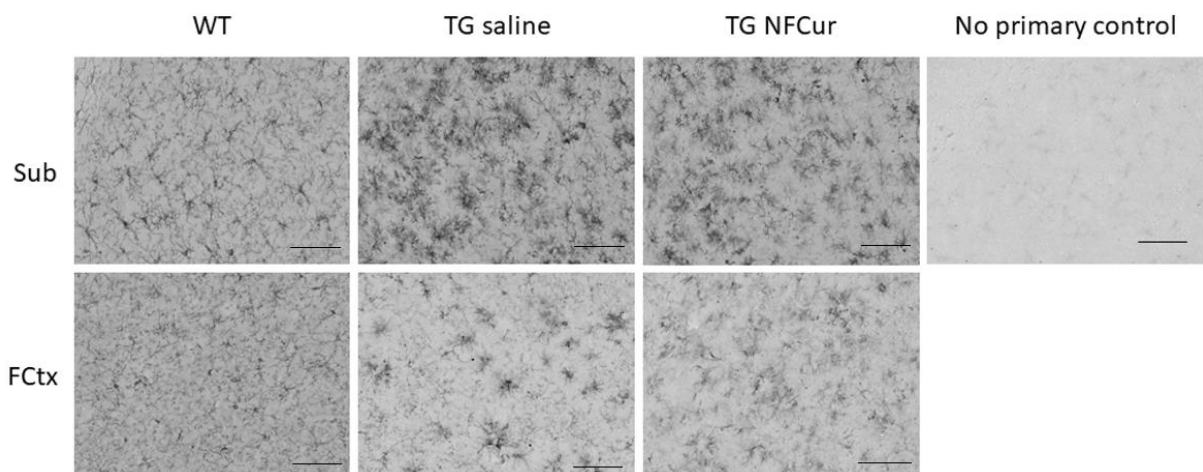


Figure 19. IBA1 immunostaining from the preclinical trial. Morphology of microglial cells in the subiculum and frontal cortex in TG mice treated with nanoformulated curcumin (TG NFcur) compared to untreated TG (TG saline) mice and WT (saline) mice. The scale bar is 100 μ m.

2.4.2 Particle analysis for the preclinical trial

Since analysing percent area did not show any significant difference between the WT and the mutants during the preclinical trial, particle analysis for analysing microglia was used (See Fig. 20) as during the pilot trial, the results were less variable than with percent analysis.

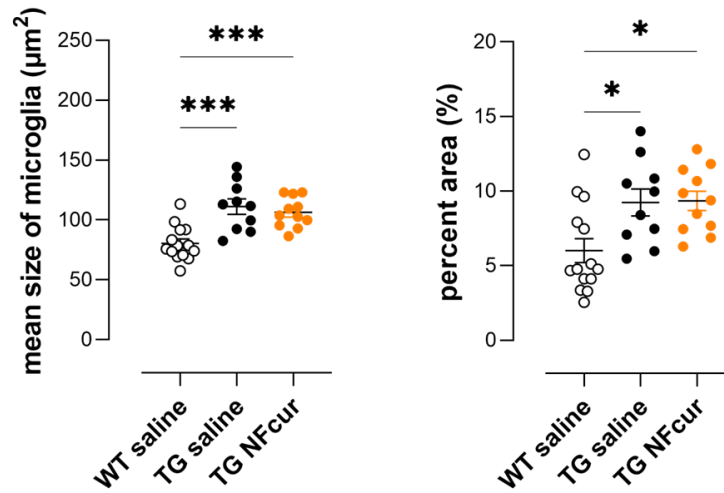


Figure 20. Microglial size and area covered by microglia with IBA1 immunostaining. N=14WT saline,10TG saline,11TG NFcur. Size and area calculated with ImageJ in 4-month-old female 5xFAD treated with nanoformulated curcumin compared with control TG and WT mice, who were treated with saline in frontal cortex and subiculum. Lines depict means. *p<0.05 ***p<0.0001

To analyse the results from the preclinical trial 1-way ANOVA and Tukey's multiple comparisons test was used. The results of the microglial size (See Fig. 20) show a significant difference between groups ($F(2, 32) = 13.66, p < 0.0001$). Tukey's multiple comparisons test revealed a strong significant difference between the WT mice and untreated TG mice ($p < 0.001$) and a strong significant difference between WT mice and TG mice treated with nanoformulated curcumin ($p < 0.001$). However, there seems to be no treatment effect as there is no significant difference between treated and untreated TG mice.

The results of the percent area covered by microglia (See Fig. 20) also revealed a significant difference between groups ($F(2, 32) = 6.166, p < 0.05$). Tukey's multiple comparisons test shows a weak significant difference between WT and untreated TG mice and between treated TG and WT mice. There is no significant difference between treated and untreated TG mice.

In conclusion, the percent area analysis of all IBA1 stained area was not sufficiently sensitive to detect large effects (WT vs TG) due to the variability of the results. Particle analysis was sensitive enough to detect a significant difference between WT and TG mice. Particle analysis was also more time sufficient than percent analysis, since a lot of the particle analysis was done automatically, thus eliminating human error as well. However, based on particle analysis of the preclinical trial, nanoformulated curcumin does not seem to have an effect on microglial cells as there was no significant difference between treated and untreated TG mice.

CONCLUSION

The literature review of this thesis gives an overview of the pathology that is involved in AD and provides an overview of current research and testing of treatment. It sheds light into problematic areas in preclinical trials.

The aim on the experimental part of this thesis was to determine the best endpoints to use in a preclinical trial for a mouse model of AD (5xFAD). This was achieved by determining appropriate behavioural endpoints, effect sizes and group sizes, that could be used to detect a treatment effect of nanoformulated curcumin on AD. The data obtained shows that Y-maze test is not sensitive enough to detect differences between WT and TG mice and should not be used in the preclinical trial. Future work could include testing a different behavioural endpoint, for example Morris water maze. The neuropathological analysis shows that even though percent area seemed to be a good endpoint in the pilot trial as there were significant differences between WT and TG mice, the results were too variable, and a genotype effect was not detected during the preclinical trial. Particle analysis was also sensitive enough to detect a strong significant difference between the WT and TG mice in the pilot trial. Furthermore, particle analysis was less variable than percent analysis, giving more consistent results and thus, making it more reliable. During the preclinical trial particle analysis proved to be the best endpoint, since it shows a significant difference between WT and treated TG mice and between WT and untreated TG mice. However, there is no difference between treated and untreated TG mice, which means that based on the particle analysis, nanoformulation of curcumin does not seem to have an effect on microglial cells at this age and with this endpoint.

The objectives of this thesis were fulfilled, and the main conclusion is that from the different endpoints analysed in this thesis, particle analysis measuring microglia is the best endpoint to use in a preclinical trial of 5xFAD mice to see a treatment effect. Future work could include the analysis of other brain areas with the same groups or same brain areas with different groups of mice. Mice could be tested at a different age and other analysis options could be tested for more information.

KOKKUVÕTE

Prekliinilistes uuringutes kasutatavate tulemusnäitajate valimine Alzheimeri tõve hiiremudelil

Alzheimeri tõbi on kõige tavalisem neurodegeneratiivne haigus ja samuti põhiline dementsuse põhjustaja tänapäeva ühiskonnas. Alzheimeri tõbi avaldub tavaliselt vanaduses (65+ eluaastat), kuid arvatakse et neurodegeneratsioon algab umbes 20-30 aastat enne kliiniliste sümptomite avaldumist, mistõttu jõuab haigus enne diagnoosimist progresseeruda kaugemale. Alzheimeri tõve arenemise peamine põhjus on β -amüloidi valgu agregaatide moodustumine ja neurofibrillarsed tängud. Alzheimeri süvenemises ja patoloogias mängib väga olulist rolli neuroinflammatsioon (Agrawal & Jha, 2020; Goedert & Spillantini, 2006). On leitud, et mikrogliaarakud on olulised neuroinflammatsiooni ja Alzheimeri tekkimises. Mikrogliaarakud asuvad kesknärvisüsteemis ja nad täidavad ajus immuunfunktsiooni eemaldades kahjustatud neuroneid ja infektsioone. Mikrogliaarakud on olulised kesknärvisüsteemi normaalses töös. Mikroglia aktiveerumine on Alzheimeri arengu üks olulisemaid mehhanisme ning nende täpsem uurimine võib viia oluliste meditsiiniliste läbimurreteni (Schwabe et al., 2020).

Selles töös kasutati hiiremudelit 5xFAD, kus on inimese APP (valgu amüloid-prekursori geen) ja PS1, PS2 (preseniliini valkude geenid) transgeenid, millel on Alzheimeri tõvega seotud viis mutatsiooni, mis suurendavad β -amüloid 42 tootmist. Transgeensed hiired ekspresseerivad neid mutatsioonidega geene ning see põhjustab käitumise ning patoloogia teket, mis on sarnane inimesega kes põeb perekondlikku (varajast) Alzheimeri tõbe (FAD, ingl *familial Alzheimer's disease*) (Oakley et al., 2006).

Käesoleva töö eesmärk on määrata sobilikud tulemusnäitajad, mida oleks võimalik kasutada prekliinilistes uuringutes kasutades 5xFAD hiiremudelit. Töö teoreetilises osas kirjeldati Alzheimeri patoloogiat ja anti ülevaade praegustest uuringutest ning potentsiaalsete ravimikandidaatide testimisest, heites valgust prekliiniliste uuringute problemaatilistele aladele. Töö praktilises osas otsiti sobilikke tulemusnäitajaid prekliinilise uuringu jaoks, nanoformuleeritud kurkumi raviefekti tuvastamiseks. Töö tulemustest on võimalik järeldada, et *Y-maze test* ei ole piisavalt tundlik transgeensete ja metsiktüüpi hiirte vahel erinevuste tuvastamiseks ja prekliinilises uuringus seda kasutada ei tohiks. Neuropatoloogiline analüüs näitab, et kuigi protsentuaalse ala analüüs tundus pilootkatses sobiva tulemusnäitajana, (oluline erinevus metsiktüüpi ja transgeensete hiire vahel) siis prekliinilises uuringus olid tulemused liiga varieeruvad ning oluline erinevus puudus eri genotüüpide vahel. Osakeste analüüsi tulemused olid pilootkatses vähem varieeruvad ning esines oluline erinevus genotüüpide vahel. Ka prekliinilises uuringus esines oluline erinevus metsiktüüpi ja ravi (kurkum) saanud transgeensete hiire vahel ning metsiktüüpi ja ravi mittesaanud transgeensete hiirte vahel.

Ravimi efektiivsus nende tulemuste põhjal mikroglia rakkude vastu puudus, sest ravi saanud ja mittesaanud transgeensete hiirte vahel olulist erinevust ei olnud.

REFERENCES

- Agrawal, I., & Jha, S. (2020). Mitochondrial Dysfunction and Alzheimer's Disease: Role of Microglia. *Frontiers in Aging Neuroscience*, 12. <https://doi.org/10.3389/fnagi.2020.00252>
- Bard, F., Cannon, C., Barbour, R., Burke, R. L., Games, D., Grajeda, H., Guido, T., Hu, K., Huang, J., Johnson-Wood, K., Khan, K., Kholodenko, D., Lee, M., Lieberburg, I., Motter, R., Nguyen, M., Soriano, F., Vasquez, N., Weiss, K., ... Yednock, T. (2000). Peripherally administered antibodies against amyloid beta-peptide enter the central nervous system and reduce pathology in a mouse model of Alzheimer disease. *Nature Medicine*, 6(8), 916–919. <https://doi.org/10.1038/78682>
- Baum, L., Lam, C. W. K., Cheung, S. K.-K., Kwok, T., Lui, V., Tsoh, J., Lam, L., Leung, V., Hui, E., & Ng, C. (2008). Six-month randomized, placebo-controlled, double-blind, pilot clinical trial of curcumin in patients with Alzheimer disease. *Journal of Clinical Psychopharmacology*, 28(1), 110–113.
- Begum, A. N., Jones, M. R., Lim, G. P., Morihara, T., Kim, P., Heath, D. D., Rock, C. L., Pruitt, M. A., Yang, F., Hudspeth, B., Hu, S., Faull, K. F., Teter, B., Cole, G. M., & Frautschy, S. A. (2008). Curcumin Structure-Function, Bioavailability, and Efficacy in Models of Neuroinflammation and Alzheimer's Disease. *Journal of Pharmacology and Experimental Therapeutics*, 326(1), 196. <https://doi.org/10.1124/jpet.108.137455>
- Bekris, L. M., Yu, C.-E., Bird, T. D., & Tsuang, D. W. (2010). Review Article: Genetics of Alzheimer Disease. *Journal of Geriatric Psychiatry and Neurology*, 23(4), 213–227. <https://doi.org/10.1177/0891988710383571>
- Bhattacharya, S., Haertel, C., Maelicke, A., & Montag, D. (2014). Galantamine slows down plaque formation and behavioral decline in the 5XFAD mouse model of Alzheimer's disease. *PloS One*, 9(2), e89454. <https://doi.org/10.1371/journal.pone.0089454>
- Bird, T. D. (2008). Genetic aspects of Alzheimer disease. *Genetics in Medicine: Official Journal of the American College of Medical Genetics*, 10(4), 231–239. <https://doi.org/10.1097/GIM.0b013e31816b64dc>
- Chen, G.-F., Xu, T.-H., Yan, Y., Zhou, Y.-R., Jiang, Y., Melcher, K., & Xu, H. E. (2017). Amyloid beta: Structure, biology and structure-based therapeutic development. *Acta Pharmacologica Sinica*, 38(9), 1205–1235. <https://doi.org/10.1038/aps.2017.28>

- Chen, J.-Y., Zhu, Q., Zhang, S., OuYang, D., & Lu, J.-H. (2019). Resveratrol in experimental Alzheimer's disease models: A systematic review of preclinical studies. *Pharmacological Research*, *150*, 104476.
- Cleal, M., Fontana, B. D., Ranson, D. C., McBride, S. D., Swinny, J. D., Redhead, E. S., & Parker, M. O. (2021). The Free-movement pattern Y-maze: A cross-species measure of working memory and executive function. *Behavior Research Methods*, *53*(2), 536–557. <https://doi.org/10.3758/s13428-020-01452-x>
- Cline, E. N., Bicca, M. A., Viola, K. L., & Klein, W. L. (2018). The Amyloid- β Oligomer Hypothesis: Beginning of the Third Decade. *Journal of Alzheimer's Disease: JAD*, *64*(s1), S567–S610. <https://doi.org/10.3233/JAD-179941>
- Cramer, P. E., Cirrito, J. R., Wesson, D. W., Lee, C. Y. D., Karlo, J. C., Zinn, A. E., Casali, B. T., Restivo, J. L., Goebel, W. D., James, M. J., Brunden, K. R., Wilson, D. A., & Landreth, G. E. (2012). ApoE-Directed Therapeutics Rapidly Clear β -Amyloid and Reverse Deficits in AD Mouse Models. *Science*, *335*(6075), 1503. <https://doi.org/10.1126/science.1217697>
- Devi, L., & Ohno, M. (2010). Phospho-eIF2 α Level Is Important for Determining Abilities of BACE1 Reduction to Rescue Cholinergic Neurodegeneration and Memory Defects in 5XFAD Mice. *PLOS ONE*, *5*(9), 1–10. <https://doi.org/10.1371/journal.pone.0012974>
- Devi, L., Tang, J., & Ohno, M. (2015). Beneficial effects of the β -secretase inhibitor GRL-8234 in 5XFAD Alzheimer's transgenic mice lessen during disease progression. *Current Alzheimer Research*, *12*(1), 13–21. <https://doi.org/10.2174/1567205012666141218125042>
- Deyts, C., Clutter, M., Pierce, N., Chakrabarty, P., Ladd, T. B., Goddi, A., Rosario, A. M., Cruz, P., Vetrivel, K., Wagner, S. L., Thinakaran, G., Golde, T. E., & Parent, A. T. (2019). APP-Mediated Signaling Prevents Memory Decline in Alzheimer's Disease Mouse Model. *Cell Reports*, *27*(5), 1345-1355.e6. <https://doi.org/10.1016/j.celrep.2019.03.087>
- Eckman, C. B., Mehta, N. D., Crook, R., Perez-tur, J., Prihar, G., Pfeiffer, E., Graff-Radford, N., Hinder, P., Yager, D., Zenk, B., Refolo, L. M., Prada, C. M., Younkin, S. G., Hutton, M., & Hardy, J. (1997). A new pathogenic mutation in the APP gene (I716V) increases the relative proportion of A beta 42(43). *Human Molecular Genetics*, *6*(12), 2087–2089. <https://doi.org/10.1093/hmg/6.12.2087>

- Egan, Kieren, & Macleod, M. (2014). Two decades testing interventions in transgenic mouse models of Alzheimer disease: Designing and interpreting studies for clinical trial success. *Clinical Investigation*, 4, 693–704. <https://doi.org/10.4155/cli.14.55>
- Egan, KJ, Vesterinen, H., Beglopoulos, V., Sena, E., & Macleod, M. (2016). From a mouse: Systematic analysis reveals limitations of experiments testing interventions in Alzheimer's disease mouse models. *Evidence-based Preclinical Medicine*, 3(1), 12–23.
- Egan, KJ, Vesterinen, H., McCann, S., Sena, E., & MacLeod, M. (2015). The development of an online database for interventions tested in transgenic mouse models of Alzheimer's disease. *Evidence-based Preclinical Medicine*, 2(1), 20–26.
- Eimer, W. A., & Vassar, R. (2013). Neuron loss in the 5XFAD mouse model of Alzheimer's disease correlates with intraneuronal A β 42 accumulation and Caspase-3 activation. *Molecular Neurodegeneration*, 8(1), 2. <https://doi.org/10.1186/1750-1326-8-2>
- Gagliardi, S., Morasso, C., Stivaktakis, P., Pandini, C., Tinelli, V., Tsatsakis, A., Prospero, D., Hickey, M., Corsi, F., & Cereda, C. (2020). Curcumin Formulations and Trials: What's New in Neurological Diseases. *Molecules*, 25(22). <https://doi.org/10.3390/molecules25225389>
- Gandy, S. (2005). The role of cerebral amyloid beta accumulation in common forms of Alzheimer disease. *The Journal of Clinical Investigation*, 115(5), 1121–1129. <https://doi.org/10.1172/JCI25100>
- Gao, C., Chu, X., Gong, W., Zheng, J., Xie, X., Wang, Y., Yang, M., Li, Z., Gao, C., & Yang, Y. (2020). Neuron tau-targeting biomimetic nanoparticles for curcumin delivery to delay progression of Alzheimer's disease. *Journal of Nanobiotechnology*, 18, 1–23.
- Gao, C., Wang, Y., Sun, J., Han, Y., Gong, W., Li, Y., Feng, Y., Wang, H., Yang, M., & Li, Z. (2020). Neuronal mitochondria-targeted delivery of curcumin by biomimetic engineered nanosystems in Alzheimer's disease mice. *Acta Biomaterialia*, 108, 285–299.
- Gauthier, S., Aisen, P., Cummings, J., Detke, M., Longo, F., Raman, R., Sabbagh, M., Schneider, L., Tanzi, R., Tariot, P., & others. (2020). Non-amyloid approaches to disease modification for Alzheimer's disease: An EU/US CTAD Task Force Report. *The Journal of Prevention of Alzheimer's Disease*, 7, 152–157.
- Goedert, M., & Spillantini, M. G. (2006). A century of Alzheimer's disease. *Science (New York, N.Y.)*, 314(5800), 777–781. <https://doi.org/10.1126/science.1132814>

- Herholz, K., & Ebmeier, K. (2011). Clinical amyloid imaging in Alzheimer's disease. *The Lancet. Neurology*, *10*(7), 667–670. [https://doi.org/10.1016/S1474-4422\(11\)70123-5](https://doi.org/10.1016/S1474-4422(11)70123-5)
- Hickey, M.A., Kosmalska, A., Enayati, J., Cohen, R., Zeitlin, S., Levine, M. S., & Chesselet, M.-F. (2008). Extensive early motor and non-motor behavioral deficits are followed by striatal neuronal loss in knock-in Huntington's disease mice. *Neuroscience*, *157*(1), 280–295. <https://doi.org/10.1016/j.neuroscience.2008.08.041>
- Hickey, Miriam A., Zhu, C., Medvedeva, V., Lerner, R. P., Patassini, S., Franich, N. R., Maiti, P., Frautschy, S. A., Zeitlin, S., Levine, M. S., & Chesselet, M.-F. (2012). Improvement of neuropathology and transcriptional deficits in CAG 140 knock-in mice supports a beneficial effect of dietary curcumin in Huntington's disease. *Molecular Neurodegeneration*, *7*, 12. <https://doi.org/10.1186/1750-1326-7-12>
- Hoover, B. R., Reed, M. N., Su, J., Penrod, R. D., Kotilinek, L. A., Grant, M. K., Pitstick, R., Carlson, G. A., Lanier, L. M., Yuan, L.-L., Ashe, K. H., & Liao, D. (2010). Tau mislocalization to dendritic spines mediates synaptic dysfunction independently of neurodegeneration. *Neuron*, *68*(6), 1067–1081. <https://doi.org/10.1016/j.neuron.2010.11.030>
- Huang, N., Lu, S., Liu, X.-G., Zhu, J., Wang, Y.-J., & Liu, R.-T. (2017). PLGA nanoparticles modified with a BBB-penetrating peptide co-delivering A β generation inhibitor and curcumin attenuate memory deficits and neuropathology in Alzheimer's disease mice. *Oncotarget*, *8*(46), 81001.
- Huang, Z., Muniz-Terrera, G., Tom, B. D. M., & Initiative, A. D. N. (2017). Power analysis to detect treatment effects in longitudinal clinical trials for Alzheimer's disease. *Alzheimer's & Dementia: Translational Research & Clinical Interventions*, *3*(3), 360–366. <https://doi.org/10.1016/j.trci.2017.04.007>
- Jansen, W. J., Ossenkoppele, R., Knol, D. L., Tijms, B. M., Scheltens, P., Verhey, F. R. J., Visser, P. J., & and the Amyloid Biomarker Study Group. (2015). Prevalence of Cerebral Amyloid Pathology in Persons Without Dementia: A Meta-analysis. *JAMA*, *313*(19), 1924–1938. <https://doi.org/10.1001/jama.2015.4668>
- Kakkar, V., & Kaur, I. P. (2011). Evaluating potential of curcumin loaded solid lipid nanoparticles in aluminium induced behavioural, biochemical and histopathological alterations in mice brain. *Food and Chemical Toxicology : An International Journal Published for the British Industrial Biological Research Association*, *49*(11), 2906–2913. <https://doi.org/10.1016/j.fct.2011.08.006>

- Khoury, R., Rajamanickam, J., & Grossberg, G. T. (2018). An update on the safety of current therapies for Alzheimer's disease: Focus on rivastigmine. *Therapeutic Advances in Drug Safety*, 9(3), 171–178. <https://doi.org/10.1177/2042098617750555>
- Kinney, J. W., Bemiller, S. M., Murtishaw, A. S., Leisgang, A. M., Salazar, A. M., & Lamb, B. T. (2018). Inflammation as a central mechanism in Alzheimer's disease. *Alzheimer's & Dementia: Translational Research & Clinical Interventions*, 4(1), 575–590. <https://doi.org/10.1016/j.trci.2018.06.014>
- Levy-Lahad, E., Wasco, W., Poorkaj, P., Romano, D. M., Oshima, J., Pettingell, W. H., Yu, C. E., Jondro, P. D., Schmidt, S. D., & Wang, K. (1995). Candidate gene for the chromosome 1 familial Alzheimer's disease locus. *Science (New York, N.Y.)*, 269(5226), 973–977. <https://doi.org/10.1126/science.7638622>
- Li, L., Fang, C. J., Ryan, J. C., Niemi, E. C., Lebrón, J. A., Björkman, P. J., Arase, H., Torti, F. M., Torti, S. V., Nakamura, M. C., & Seaman, W. E. (2010). Binding and uptake of H-ferritin are mediated by human transferrin receptor-1. *Proceedings of the National Academy of Sciences*, 107(8), 3505. <https://doi.org/10.1073/pnas.0913192107>
- Murphy, M. P., & LeVine, H. 3rd. (2010). Alzheimer's disease and the amyloid-beta peptide. *Journal of Alzheimer's Disease : JAD*, 19(1), 311–323. <https://doi.org/10.3233/JAD-2010-1221>
- Oakley, H., Cole, S. L., Logan, S., Maus, E., Shao, P., Craft, J., Guillozet-Bongaarts, A., Ohno, M., Disterhoft, J., Van Eldik, L., Berry, R., & Vassar, R. (2006). Intraneuronal beta-amyloid aggregates, neurodegeneration, and neuron loss in transgenic mice with five familial Alzheimer's disease mutations: Potential factors in amyloid plaque formation. *The Journal of Neuroscience : The Official Journal of the Society for Neuroscience*, 26(40), 10129–10140. <https://doi.org/10.1523/JNEUROSCI.1202-06.2006>
- Pandolfi, L., Bellini, M., Vanna, R., Morasso, C., Zago, A., Carcano, S., Avvakumova, S., Bertolini, J. A., Rizzuto, M. A., Colombo, M., & Prospero, D. (2017). H-Ferritin Enriches the Curcumin Uptake and Improves the Therapeutic Efficacy in Triple Negative Breast Cancer Cells. *Biomacromolecules*, 18(10), 3318–3330. <https://doi.org/10.1021/acs.biomac.7b00974>
- Price, A., Xu, G., Siemienski, Z., Smithson, L., Borchelt, D., & Felsenstein, K. (2013). Comment on 'ApoE-Directed Therapeutics Rapidly Clear -Amyloid and Reverse Deficits in AD Mouse Models'. *Science (New York, N.Y.)*, 340, 924. <https://doi.org/10.1126/science.1234089>

- Qiu, C., Kivipelto, M., & von Strauss, E. (2009). Epidemiology of Alzheimer's disease: Occurrence, determinants, and strategies toward intervention. *Dialogues in Clinical Neuroscience, 11*(2), 111–128. PubMed.
- Rahman, S. O., Hussain, S., Alzahrani, A., Akhtar, M., & Najmi, A. K. (2020). Effect of statins on amyloidosis in the rodent models of Alzheimer's disease: Evidence from the preclinical meta-analysis. *Brain Research, 147115*.
- Reddy, P. H., Manczak, M., Yin, X., Grady, M. C., Mitchell, A., Kandimalla, R., & Kuruva, C. S. (2016). Protective effects of a natural product, curcumin, against amyloid β induced mitochondrial and synaptic toxicities in Alzheimer's disease. *Journal of Investigative Medicine, 64*(8), 1220. <https://doi.org/10.1136/jim-2016-000240>
- Ringman, J. M., Frautschy, S. A., Teng, E., Begum, A. N., Bardens, J., Beigi, M., Gylys, K. H., Badmaev, V., Heath, D. D., & Apostolova, L. G. (2012). Oral curcumin for Alzheimer's disease: Tolerability and efficacy in a 24-week randomized, double blind, placebo-controlled study. *Alzheimer's Research & Therapy, 4*(5), 1–8.
- Rodríguez-Martín, T., Cuchillo-Ibáñez, I., Noble, W., Nyenya, F., Anderton, B. H., & Hanger, D. P. (2013). Tau phosphorylation affects its axonal transport and degradation. *Neurobiology of Aging, 34*(9), 2146–2157. <https://doi.org/10.1016/j.neurobiolaging.2013.03.015>
- Rohn, T. (2013). The Triggering Receptor Expressed on Myeloid Cells 2: “TREM-ming” the Inflammatory Component Associated with Alzheimer's Disease. *Oxidative Medicine and Cellular Longevity, 2013*, 860959. <https://doi.org/10.1155/2013/860959>
- Sasaguri, H., Nilsson, P., Hashimoto, S., Nagata, K., Saito, T., De Strooper, B., Hardy, J., Vassar, R., Winblad, B., & Saido, T. C. (2017). APP mouse models for Alzheimer's disease preclinical studies. *The EMBO Journal, 36*(17), 2473–2487. <https://doi.org/10.15252/embj.201797397>
- Schachter, A. S., & Davis, K. L. (2000). Alzheimer's disease. *Dialogues in Clinical Neuroscience, 2*(2), 91–100. <https://doi.org/10.31887/DCNS.2000.2.2/asschachter>
- Scheltens, P., Blennow, K., Breteler, M. M. B., de Strooper, B., Frisoni, G. B., Salloway, S., & Van der Flier, W. M. (2016a). Alzheimer's disease. *The Lancet, 388*(10043), 505–517. [https://doi.org/10.1016/S0140-6736\(15\)01124-1](https://doi.org/10.1016/S0140-6736(15)01124-1)

- Schwabe, T., Srinivasan, K., & Rhinn, H. (2020). Shifting paradigms: The central role of microglia in Alzheimer's disease. *Neurobiology of Disease*, *143*, 104962. <https://doi.org/10.1016/j.nbd.2020.104962>
- Selkoe, D. J. (2001). Alzheimer's disease: Genes, proteins, and therapy. *Physiological Reviews*, *81*(2), 741–766. <https://doi.org/10.1152/physrev.2001.81.2.741>
- Serrano-Pozo, A., Frosch, M. P., Masliah, E., & Hyman, B. T. (2011). Neuropathological alterations in Alzheimer disease. *Cold Spring Harbor Perspectives in Medicine*, *1*(1), a006189. <https://doi.org/10.1101/cshperspect.a006189>
- Shahryari, V., Nip, H., Saini, S., Dar, A. A., Yamamura, S., Mitsui, Y., Colden, M., Bucay, N., Tabatabai, L. Z., Greene, K., Deng, G., Tanaka, Y., Dahiya, R., & Majid, S. (2016). Pre-clinical Orthotopic Murine Model of Human Prostate Cancer. *Journal of Visualized Experiments : JoVE*, *114*. <https://doi.org/10.3791/54125>
- Sherrington, R., Rogaev, E. I., Liang, Y., Rogaeva, E. A., Levesque, G., Ikeda, M., Chi, H., Lin, C., Li, G., Holman, K., Tsuda, T., Mar, L., Foncin, J. F., Bruni, A. C., Montesi, M. P., Sorbi, S., Rainero, I., Pinessi, L., Nee, L., ... St George-Hyslop, P. H. (1995). Cloning of a gene bearing missense mutations in early-onset familial Alzheimer's disease. *Nature*, *375*(6534), 754–760. <https://doi.org/10.1038/375754a0>
- Shi, J., Sabbagh, M. N., & Vellas, B. (2020). Alzheimer's disease beyond amyloid: Strategies for future therapeutic interventions. *BMJ*, *371*. <https://doi.org/10.1136/bmj.m3684>
- Shineman, D. W., Basi, G. S., Bizon, J. L., Colton, C. A., Greenberg, B. D., Hollister, B. A., Lincecum, J., Leblanc, G. G., Lee, L. B. H., Luo, F., Morgan, D., Morse, I., Refolo, L. M., Riddell, D. R., Scarce-Levie, K., Sweeney, P., Yrjänheikki, J., & Fillit, H. M. (2011). Accelerating drug discovery for Alzheimer's disease: Best practices for preclinical animal studies. *Alzheimer's Research & Therapy*, *3*(5), 28. <https://doi.org/10.1186/alzrt90>
- Shukla, V., Zheng, Y.-L., Mishra, S., Amin, N., Steiner, J., Grant, P., Kesavapany, S., & Pant, H. (2012). A truncated peptide from p35, a Cdk5 activator, prevents Alzheimer's disease phenotypes in model mice. *FASEB Journal : Official Publication of the Federation of American Societies for Experimental Biology*, *27*. <https://doi.org/10.1096/fj.12-217497>
- Song, W. M., Joshita, S., Zhou, Y., Ulland, T. K., Gilfillan, S., & Colonna, M. (2018). Humanized TREM2 mice reveal microglia-intrinsic and -extrinsic effects of R47H polymorphism. *Journal of Experimental Medicine*, *215*(3), 745–760. <https://doi.org/10.1084/jem.20171529>

- Sosna, J., Philipp, S., Albay, R., Reyes-Ruiz, J. M., Baglietto-Vargas, D., LaFerla, F. M., & Glabe, C. G. (2018). Early long-term administration of the CSF1R inhibitor PLX3397 ablates microglia and reduces accumulation of intraneuronal amyloid, neuritic plaque deposition and pre-fibrillar oligomers in 5XFAD mouse model of Alzheimer's disease. *Molecular Neurodegeneration*, *13*(1), 11. <https://doi.org/10.1186/s13024-018-0244-x>
- Tesseur, I., Lo, A. C., Roberfroid, A., Dietvorst, S., Van Broeck, B., Borgers, M., Gijzen, H., Moechars, D., Mercken, M., Kemp, J., D'Hooge, R., & De Strooper, B. (2013). Comment on "ApoE-Directed Therapeutics Rapidly Clear β -Amyloid and Reverse Deficits in AD Mouse Models". *Science*, *340*(6135), 924–924. <https://doi.org/10.1126/science.1233937>
- Tiwari, S., Atluri, V., Kaushik, A., Yndart, A., & Nair, M. (2019). Alzheimer's disease: Pathogenesis, diagnostics, and therapeutics. *International Journal of Nanomedicine*, *14*, 5541–5554. <https://doi.org/10.2147/IJN.S200490>
- Torres-Platas, S. G., Comeau, S., Rachalski, A., Bo, G. D., Cruceanu, C., Turecki, G., Giros, B., & Mechawar, N. (2014). Morphometric characterization of microglial phenotypes in human cerebral cortex. *Journal of Neuroinflammation*, *11*(1), 12. <https://doi.org/10.1186/1742-2094-11-12>
- van der Kant, R., Goldstein, L. S. B., & Ossenkoppele, R. (2020). Amyloid- β -independent regulators of tau pathology in Alzheimer disease. *Nature Reviews Neuroscience*, *21*(1), 21–35. <https://doi.org/10.1038/s41583-019-0240-3>
- Vorhees, C. V., & Williams, M. T. (2006). Morris water maze: Procedures for assessing spatial and related forms of learning and memory. *Nature Protocols*, *1*(2), 848–858. <https://doi.org/10.1038/nprot.2006.116>
- Weiner, M. W., Veitch, D. P., Aisen, P. S., Beckett, L. A., Cairns, N. J., Cedarbaum, J., Green, R. C., Harvey, D., Jack, C. R., Jagust, W., Luthman, J., Morris, J. C., Petersen, R. C., Saykin, A. J., Shaw, L., Shen, L., Schwarz, A., Toga, A. W., Trojanowski, J. Q., & Alzheimer's Disease Neuroimaging Initiative. (2015). 2014 Update of the Alzheimer's Disease Neuroimaging Initiative: A review of papers published since its inception. *Alzheimer's & Dementia : The Journal of the Alzheimer's Association*, *11*(6), e1–e120. PubMed. <https://doi.org/10.1016/j.jalz.2014.11.001>
- Weller, J., & Budson, A. (2018). Current understanding of Alzheimer's disease diagnosis and treatment. *F1000Research*, *7*, F1000 Faculty Rev-1161. PubMed. <https://doi.org/10.12688/f1000research.14506.1>

- Wendt, S., Maricos, M., Vana, N., Meyer, N., Guneykaya, D., Semtner, M., & Kettenmann, H. (2017). Changes in phagocytosis and potassium channel activity in microglia of 5xFAD mice indicate alterations in purinergic signaling in a mouse model of Alzheimer's disease. *Neurobiology of Aging*, 58, 41–53. <https://doi.org/10.1016/j.neurobiolaging.2017.05.027>
- Wenk, G. L. (2003). Neuropathologic changes in Alzheimer's disease. *The Journal of Clinical Psychiatry*, 64 Suppl 9, 7–10.
- Whiley, L., Chappell, K. E., D'Hondt, E., Lewis, M. R., Jiménez, B., Snowden, S. G., Soininen, H., Kłoszewska, I., Mecocci, P., Tsolaki, M., Vellas, B., Swann, J. R., Hye, A., Lovestone, S., Legido-Quigley, C., Holmes, E., Soininen, H., Kłoszewska, I., Mecocci, P., ... on behalf of AddNeuroMed consortium. (2021). Metabolic phenotyping reveals a reduction in the bioavailability of serotonin and kynurenine pathway metabolites in both the urine and serum of individuals living with Alzheimer's disease. *Alzheimer's Research & Therapy*, 13(1), 20. <https://doi.org/10.1186/s13195-020-00741-z>
- Wolf, A., Bauer, B., Abner, E. L., Ashkenazy-Frolinger, T., & Hartz, A. M. S. (2016). A Comprehensive Behavioral Test Battery to Assess Learning and Memory in 129S6/Tg2576 Mice. *PloS One*, 11(1), e0147733–e0147733. PubMed. <https://doi.org/10.1371/journal.pone.0147733>
- Wolfe, M. S. (2007). When loss is gain: Reduced presenilin proteolytic function leads to increased Aβ₄₂/Aβ₄₀. Talking Point on the role of presenilin mutations in Alzheimer disease. *EMBO Reports*, 8(2), 136–140. <https://doi.org/10.1038/sj.embor.7400896>
- Zhang, X.-W., Chen, J.-Y., Ouyang, D., & Lu, J.-H. (2020). Quercetin in animal models of Alzheimer's disease: A systematic review of preclinical studies. *International Journal of Molecular Sciences*, 21(2), 493.
- Zhao, L. N., Lu, L., Chew, L. Y., & Mu, Y. (2014). Alzheimer's disease—A panorama glimpse. *International Journal of Molecular Sciences*, 15(7), 12631–12650. PubMed. <https://doi.org/10.3390/ijms150712631>
- Young, K., & Morrison, H., 2018. „Quantifying Microglia Morphology from Photomicrographs of Immunohistochemistry Prepared Tissue Using ImageJ“. *JoVE*, nr 136 (June): e57648. <https://doi.org/10.3791/57648>.

INTERNET REFERENCES

Kane SP. Sample Size Calculator. ClinCalc: <https://clincalc.com/stats/samplesize.aspx>.
Updated July 24, 2019. Accessed March 3, 2021.

ACKNOWLEDGMENTS

I would like to express my sincere gratitude to my supervisor Dr Miriam A Hickey for their assistance at every stage of my thesis and experiments. I appreciate all their insightful comments, suggestions, continuous support, and patience. I would also like to thank my co-supervisor Dr Tambet Tõnissoo for valuable advice on the editing and finalising of my thesis.

NON-EXCLUSIVE LICENCE

Non-exclusive licence to reproduce thesis and make thesis public

I, Jana Aid,

1. herewith grant the University of Tartu a free permit (non-exclusive licence) to:
 - 1.1. reproduce, for the purpose of preservation, including for adding to the DSpace digital archives until the expiry of the term of copyright, and
 - 1.2. make available to the public via the web environment of the University of Tartu, including via the DSpace digital archives, under the Creative Commons licence CC BY NC ND 3.0, which allows, by giving appropriate credit to the author, to reproduce, distribute the work and communicate it to the public, and prohibits the creation of derivative works and any commercial use of the work from **31/05/2023** until the expiry of the term of copyright,

Selecting endpoints to use in preclinical trials in a mouse model of Alzheimer's disease,

supervised by Miriam Ann Hickey and Tambet Tõnissoo,

2. I am aware of the fact that the author retains the rights specified in p. 1.
3. I certify that granting the non-exclusive licence does not infringe other persons' intellectual property rights or rights arising from the personal data protection legislation.

Jana Aid

31/05/2021